doi:10.11887/j.issn.1001-2486.26010014 http://journal.nudt.edu.cn

基于二维材料的前沿技术研究进展与展望

蔡 晗[1],轩啸宇[2*],贺彦超[3],冯薪谕[3],秦 文[1],朱熠奇[1],张尔文[1],陈文发[1],易 敏[1],刘衍朋[1],刘 政[3*],张助华[1*]

(1. 南京航空航天大学 航空航天结构力学及控制全国重点实验室,江苏 南京 210016;2. 南京航空航天大学 航空学院,江苏 南京 210016;3. 南洋理工大学 材料科学与工程学院,新加坡 新加坡 639798)

摘 要:针对航空航天及高端特种装备中传统材料日益逼近物理极限,难以兼顾"尺寸、重量、功耗"严苛要求的重大挑战,聚焦二维材料这一前沿方向,系统阐述其凭借原子级厚度与量子限域效应所带来的应用潜力。通过系统综述二维材料在隐身与电磁屏蔽(生存力)、高性能传感与探测(感知力)、轻量化防护与防腐(防御力)、高效能源与动力(保障力)及量子技术与信息安全(计算力)等核心领域的最新进展,揭示了其微观性能与宏观效能之间的内在关联与作用机制。深入剖析了当前二维材料走向工程化应用的关键瓶颈,包括晶圆级高质量制备、极端环境长期稳定性以及检测评价标准化等核心难题。结合人工智能辅助设计、异质结堆叠等新兴技术,进一步展望了面向下一代智能特种装备的基于二维材料多功能集成与智能响应系统的发展趋势,旨在为抢占未来技术制高点提供理论支撑与前瞻性参考。

关键词:二维材料;前沿材料;隐身与屏蔽;智能传感;高效储能;高端装备

中图分类号:TB383.1 **文献标志码**:A **文章编号**:1001-2486(2026)03-141-21

Research progress and prospects of frontier technologies based on two-dimensional materials

CAI Han[1], *XUAN Xiaoyu*[2*], *HE Yanchao*[3], *FENG Xinyu*[3], *QIN Wen*[1], *ZHU Yiqi*[1], *ZHANG Erwen*[1], *CHEN Wenfa*[1], *YI Min*[1], *LIU Yanpeng*[1], *LIU Zheng*[3*], *ZHANG Zhuhua*[1*]

(1. State Key Laboratory of Mechanics and Control for Mechanical Structures, Nanjing University of Aeronautics and Astronautics, Nanjing 210016, China;
2. College of Aerospace Engineering, Nanjing University of Aeronautics and Astronautics, Nanjing 210016, China;
3. School of Materials Science and Engineering, Nanyang Technological University, Singapore 639798, Singapore)

Abstract: To address the critical challenges where traditional materials in aerospace and high-end advanced equipment are approaching their physical limits and struggling to meet the stringent SWaP (size, weight and power) requirements, the frontier of 2D (two-dimensional) materials is the primary focus. This paper systematically elucidated their application potential, derived from their atomic-level thickness and quantum confinement effects. By comprehensively reviewing the latest advancements in five core areas—stealth and electromagnetic shielding (survivability), high-performance sensing and detection (perception), lightweight protection and anti-corrosion (defense), high-efficiency energy and power (logistics/support), and quantum technology and information security (computing)—it revealed the intrinsic correlations and mechanisms connecting microscopic properties to macroscopic performance. Furthermore, the key bottlenecks restricting the engineering implementation of 2D materials were analyzed, including wafer-scale high-quality fabrication, long-term stability in extreme environments, and the standardization of testing and evaluation. Based on this analysis, and incorporating emerging technologies such as AI (artificial intelligence)-assisted design and heterostructure stacking, an outlook was presented for achieving multi-functional integration and intelligent systems based on 2D materials towards the development of next-generation smart equipment. This review aims to provide theoretical support and forward-looking insights for securing a strategic technological edge in the future.

Keywords: 2D materials; frontier materials; stealth and shielding; intelligent sensing; high-efficiency energy storage; high-end equipment

收稿日期:2026-01-09

基金项目:教育部基础学科与交叉学科突破计划资助项目(JYB2025XDXM205);国家重点研发计划资助项目(2024YFA1409600);国家自然科学基金资助项目(12225205,U2441272,12261160367);江苏省基础研究计划资助项目(BK20253025)

第一作者:蔡晗(1999—),男,江苏宿迁人,博士研究生,E-mail:imcaihan@nuaa.edu.cn

***通信作者**:轩啸宇(1990—),男,河南商丘人,助理研究员,博士,E-mail:xuanyuanxy@nuaa.edu.cn

刘政(1983—),男,湖北赤壁人,教授,博士,博士生导师,E-mail:z.liu@ntu.edu.sg

张助华(1983—),男,江西九江人,教授,博士,博士生导师,E-mail:chuwazhang@nuaa.edu.cn

引用格式:蔡晗,轩啸宇,贺彦超,等. 基于二维材料的前沿技术研究进展与展望[J]. 国防科技大学学报,2026,48(3):141-161.

Citation: CAI H, XUAN X Y, HE Y C, et al. Research progress and prospects of frontier technologies based on two-dimensional materials[J]. Journal of National University of Defense Technology, 2026, 48(3): 141-161.

当前,新一轮科技革命与产业革命正推动装备形态向信息化、智能化与多域融合方向加速演进。从高超声速飞行器的热障突破到深海精密探测的极限灵敏度,现代前沿装备科技对材料性能的要求已逼近传统三维块体材料的物理极限。当下,“摩尔定律”放缓,传统半导体热耗散瓶颈凸显,高端制造领域亟须寻找一种能打破传统“结构 - 性能”权衡关系的新型物质载体。二维材料凭借其原子级厚度与独特的量子效应[1-6],为重塑特种装备的“尺寸、重量、功耗”(size, weight and power,SWaP)指标提供了颠覆性范式,成为引领装备向微型化、智能化与多功能化变革,并抢占未来科技制高点的关键材料体系。从超高灵敏红外探测到下一代隐身涂层,从超强韧抗冲击材料到颠覆性量子信息器件,其在科技前沿的应用正以前所未有的速度拓展,为未来战略优势的重塑和装备发展范式升级提供全新的物质基础。

二维材料的前沿技术价值根植于其低维结构引发的独特物理机制,与特种装备对材料性能的极端要求高度契合。首先,量子限域效应会引发电子能带重构。以过渡金属二硫属化合物[7](transition metal dichalcogenides,TMDs)中的 MoS_2 为例,当其从体材料减薄至单层时,会经历从间接带隙向直接带隙的转变[8-9],光致发光效率显著提升,其光响应可覆盖从可见光到近红外波段,为光电探测奠定基础。其次,原子级超高比表面积赋予其极高的表面活性与吸附能力,使其能捕捉微弱化学或电磁信号,完美契合高危环境预警需求。再者,石墨烯的狄拉克半金属电子结构赋予其超高载流子迁移率(1×10^6 $cm^2/(V \cdot s)$)[10],但其性能极度依赖基底环境,而作为绝缘层的六方氮化硼(hexagonal boron nitride, h-BN)则拥有优异的声子传导能力(400 W/(m · K))[11-13],两者结合为高功率雷达和电子芯片的“速率 - 散热”矛盾提供了协同解决方案。此外,二维材料体系中的单光子发射、层间反磁耦合以及自旋 - 能谷锁定等新颖的量子效应[14],更为开发抗干扰的量子通信技术开辟了新维度。

上述特性使得二维材料家族构成了前沿技术应用的丰富“武器库”。以石墨烯[15-16]、硼烯[17]为代表的单质类,凭借卓越的力学性能(如石墨烯凭借 sp^2 杂化带来的 130 GPa 超高强度[16])与高导电性[18],成为轻量化装甲与隐身涂层的首选。以 TMDs 为代表的化合物二维材料,依靠范德华力堆叠“原子级乐高”形成多层异质结,在抗辐射加固芯片与柔性电子领域展现出超越硅基极限的潜力[15]。而类似 CrI_3 这类本征磁性二维材料,则为构筑高密度、超快响应的自旋存储与信息器件提供了理想平台[19-20]。这些材料通过改变层间转角等方式调控能带,可实现光电、磁电等特种功能的“按需定制”,极大扩展了其应用灵活性。

尽管现有文献已对二维材料制备与基础物性有了深入探讨[11, 16, 21-24],但鲜有从工程应用视角对高端特种装备紧迫需求进行系统论述。本文将立足于此,聚焦隐身与电磁屏蔽(生存力)、高性能传感与探测(感知力)、轻量化防护与防腐(防御力)、高效能源与动力(保障力)、量子技术与信息安全(计算力)五大维度(如图 1 所示),系统梳理二维材料的最新进展,剖析其应用潜力,厘清当前工程化面临的关键挑战,并最终展望其在未来智能装备体系中的发展趋势。

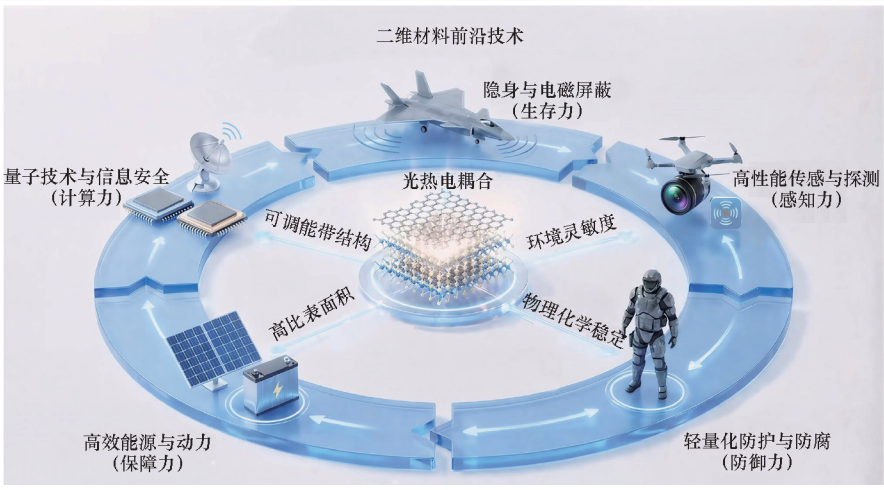

图 1 二维材料在前沿领域的潜在应用

Fig. 1 Potential applications of 2D materials in frontier fields

1　国内外进展

1.1　隐身与电磁屏蔽

在信息化、智能化背景下,隐身与电磁屏蔽能力已成为衡量现代装备性能的关键指标。无论是雷达波、红外波还是声波,实现隐身与屏蔽的关键都在于界面阻抗匹配与内部能量损耗。通过谐调材料参数使其输入阻抗与环境匹配,引导入射波最大限度进入材料内部而非反射;随后,利用材料的共振吸收、干涉相消等特性实现能量的高效衰减,从而实现复杂环境下装备的隐身与电磁屏蔽[25-26]。面对多波段侦察与复杂电磁环境中的干扰与压制,单一手段难以满足作战需求,因此,多频段一体化隐身/防护成为重要方向。得益于原子级厚度与优异的光电及声学可调性,二维材料为实现该目标提供了全新路径。近年来,相关研究主要围绕电磁干扰(electromagnetic interference, EMI)屏蔽、雷达隐身(微波/毫米波吸收)、红外隐身(热伪装)以及声学隐身(水下吸声)展开,如图 2 所示[27-33]。下文将依次评述其重要进展。

1.1.1　电磁干扰屏蔽

针对高频电路的电磁兼容(electromagnetic compatibility,EMC)需求,石墨烯材料利用其高导电网络产生的反射与吸收奠定了早期技术基础。Liang 等率先利用原位工艺制备了氧化还原石墨烯/环氧树脂复合材料,在约 1 000 S/cm 电导率下实现 21 dB 的有效屏蔽[34];随后 Han 等验证了石墨烯对电磁波的高效吸收性能,进一步考量了其电磁屏蔽能力[35];此外多个研究团队揭示了石墨烯的层数与电磁屏蔽能力密切相关[27, 36-37]。为进一步扩展防护频域至太赫兹(THz)波段,少

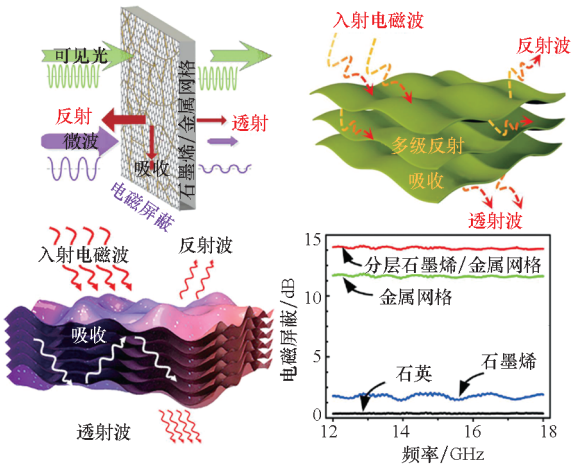

(a) 基于二维材料的电磁干扰屏蔽材料[27-29]

(a) 2D material-based EMI shielding materials[27-29]

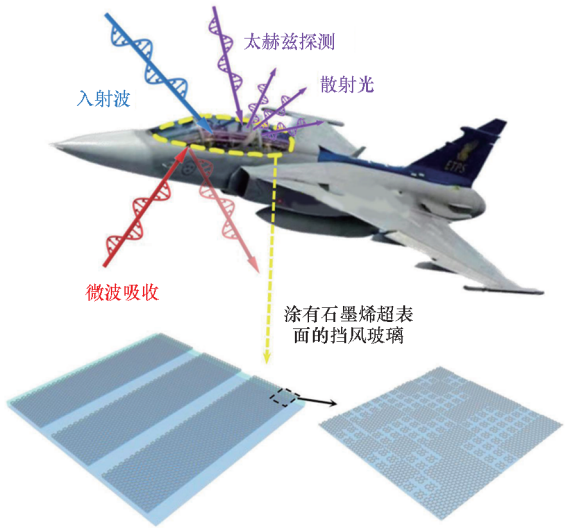

(b) 用于航天器挡风玻璃的二维材料超表面吸波器[30]

(b) 2D material metasurface absorber for spacecraft windshields[30]

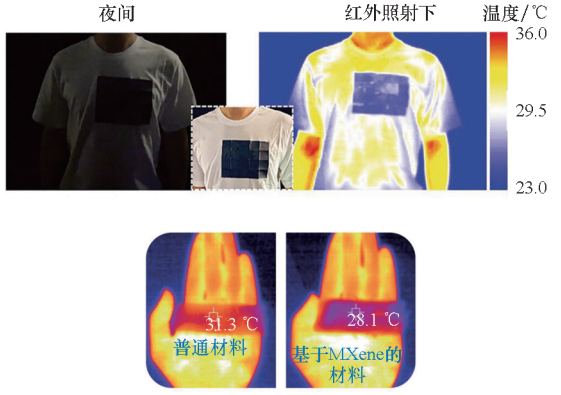

(c) 用于红外热伪装的二维材料[31-32]

(c) 2D materials for infrared thermal camouflage[31-32]

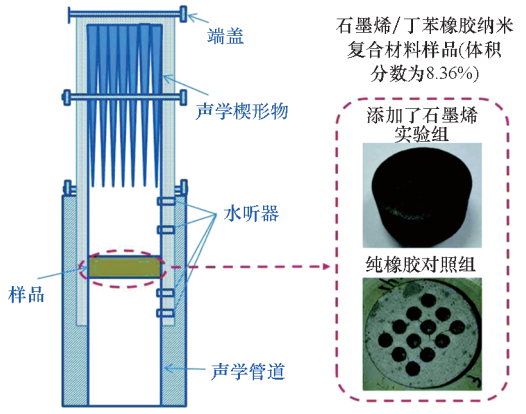

(d) 通过二维材料增强水下吸声能力的复合材料[33]

(d) 2D material-enhanced underwater sound absorbing composites[33]

图 2　二维材料助力装备多频段隐身与电磁屏蔽

Fig. 2　2D materials enabling multi-band stealth and electromagnetic shielding of equipment

层硼烯被证实表现卓越，在 0.1 ~ 2.7 THz 范围内屏蔽效能可达 50 ~ 70 dB[38-40]。二维过渡金属碳化物/氮化物(MXene)材料则凭借其广阔的电导率调控空间(5 ~ 20 000 S/cm)展现出媲美金属薄膜的屏蔽潜力[28-29, 41]。研究表明，无论是经过退火处理、构筑层间结构还是利用本征高导特性，MXene 均能在亚毫米级甚至更薄厚度下稳定实现 67.3 ~ 76.1 dB 的屏蔽效能[29, 42]。因此，上述二维材料凭借薄层和结构设计，能够实现轻量化的高效电磁屏蔽。

1.1.2 雷达隐身

在雷达隐身方面，利用吸波手段有效减小目标的雷达散射截面是主流技术路径[30]。2012 年，Thongrattanasiri 等利用石墨烯图案化设计实现了波的“完美吸收”[43]。此后，研究者们开始利用石墨烯柔性层状结构的特征构建多层/梯度超表面等复杂堆叠，以拓宽吸收带宽[44-46]；石墨烯制备方法的多样性也进一步增强了吸波可调性[47-49]。此外，石墨化氮化碳、MoS_2 和 WS_2 等二维材料通过复合结构设计，在微波吸收领域同样具备应用前景[50-52]。因此，二维材料的优异特性使得其具备“可调谐”隐身/吸波的工程潜力。

1.1.3 红外隐身

到了红外波段，隐身的核心在于降低 8 ~ 14 μm 大气窗口内的发射率以实现热伪装。$Ti_3C_2T_x$ 等 MXene 材料凭借约 0.19 的本征低发射率[31-32, 53-54]和结构可调性，为自适应隐身奠定了基础。此外，研究指出，$MoSe_2$ 兼具本征低发射率和高反射率(>75%)及良好的高温稳定性[55]，从而进一步验证了二维材料在复杂工况下实现长效红外隐身的工程潜力。

1.1.4 声学隐身

除了电磁波段外，针对水下声学信号的管控也至关重要。石墨烯复合材料凭借优异的阻尼特性显著提升了吸声效能[33, 56-58]，仅需10 phr填充量即可将基体的平均吸声系数从 0.35 提升至 0.73。Fu 验证了其在高静水压力下的吸声稳定性[41]；Li 等则利用多层叠加结构设计实现了宽频域定制化高效吸收(>90%)[59]，为应对变频水声探测提供了灵活的频谱匹配策略。

然而，尽管二维材料在此领域展现出广阔的前景，但其环境稳定性和大面积可控制备仍面临基础技术层面的挑战，制约了相关器件研究的深入开展。未来有必要进一步攻克相关高质量制备和封装难题，在复杂环境下实现微波、红外、声学等多波段的协同隐身，提升装备在服役时的生存能力与任务适配性。

1.2 高性能传感与探测

现代复杂信息环境对瞬息万变的现场监测提出了更高要求。二维材料凭借原子层厚度带来的超高比表面积、可调电子能带结构及优异的柔性，构筑了独特的界面高敏感性与多物理场耦合机制：利用界面电荷转移实现对极微量分子的场效应调制，或是利用压阻效应将微小形变转化为电信号输出。这种多维感测能力为突破传统传感器在检测极限、集成度和环境适应性方面的瓶颈提供了革命性路径。它们在高危化学/生物制剂微量检测、柔性应力/应变监测、高速宽谱光电探测以及先进医疗检测等(如图 3 所示[60-63])前沿技术领域展现出了不可替代的战略价值。

1.2.1 高危化学/生物制剂检测

针对沙林、维埃克斯及硫芥子气等高毒性化合物的早期预警是防化领域的重点[64-65]。相较

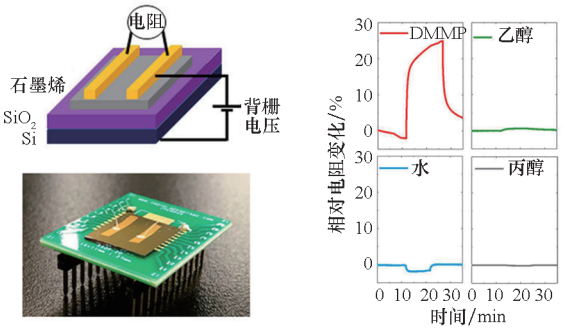

(a) 石墨烯场效应晶体管沙林探测器[60]

(a) Graphene field-effect transistor sarin detector[60]

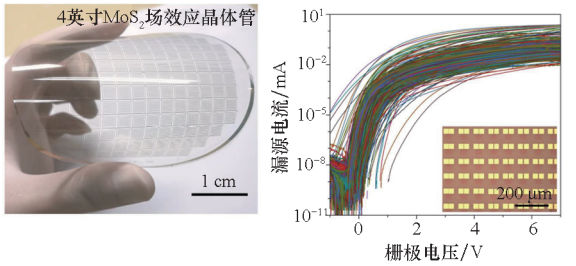

(b) 单层 MoS_2 低功耗柔性集成电路[61]

(b) Monolayer MoS_2 low-power flexible integrated circuits[61]

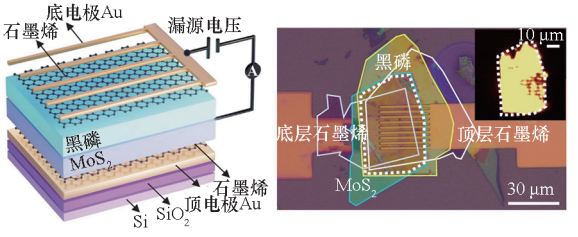

(c) 范德华异质结红外探测器[62]

(c) Van der Waals heterostructure infrared photodetector[62]

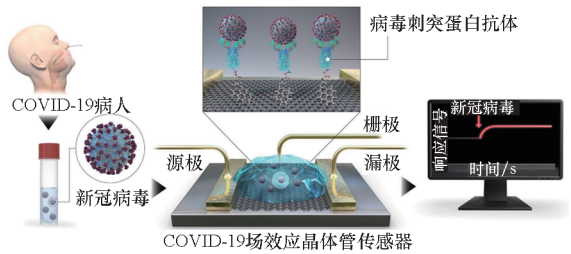

(d) 石墨烯场效应晶体管病毒生物传感器[63]

(d) Graphene field-effect transistor virus biosensor[63]

图 3　二维材料用于检测和探测

Fig. 3　Sensing and detection applications of 2D materials

于受限于灵敏度与选择性的传统离子迁移谱仪[65],二维材料传感器凭借室温工作、低能耗及超高灵敏度优势脱颖而出[65-67](见表 1[60,68-75])。研究表明紫外线(ultraviolet,UV)激活的石墨烯对甲基膦酸二甲酯(dimethyl methylphosphonate,DMMP)的检测极限可达 8.0×10^{-7} mol·mol^{-1}[60],经四氟氢醌功能化后其检测选择性显著增强[76];还原氧化石墨烯(reduced graphene oxide,rGO)则实现了对剧毒氰化氢(hydrogen cyanide,HCN)低至 7.0×10^{-8} mol·mol^{-1}的室温响应[75]。此外,MoS_2、WSe_2 等 TMDs 对神经毒性模拟物表现出优异的电导响应(WSe_2 对 DMMP 的检测极限可达 1.22×10^{-7} mol·mol^{-1})[68-69]。为克服本征 TMDs 易氧化及选择性不足的缺陷,Nb 掺杂等改性策略被证实能有效提升其稳定性及对沙林和硫芥子气的响应度[71]。尽管已突破 10^{-9} 量级检测,未来仍需聚焦器件在复杂工况下的长期可靠性及与互补金属氧化物半导体(complementary metal oxide semiconductor,CMOS)工艺兼容的异质集成难题。

表 1　二维材料对剧毒化学品与生物标识物的检测性能

Tab. 1　Detection performance of 2D materials for highly toxic chemicals and biomarkers

材料	传感平台	工作温度	检测目标	检测极限	响应时间	响应指标[a]	参考文献
MoS_2 单层	场效应晶体管(field effect transistor,FET)	室温	V 系神经毒素分解产物	1.0×10^{-8} mol·mol^{-1}	—	可逆的电导增加	[68]
WSe_2 纳米片	化学电阻	室温	DMMP	≈1.22×10^{-7} mol·mol^{-1}	100 s	10^{-4} mol·mol^{-1}时 $\Delta R/R_0=8.91\%$	[69]
WS_2 薄膜	石英晶体微天平(quartz crystal microbalance,QCM)	室温	DMMP	5.0×10^{-3} mol·mol^{-1}	—	—	[70]
Nb 掺杂 MoS_2 纳米片	化学电阻	室温	沙林、硫芥子气	0.05 mg·m^{-3}	78 s(沙林);30s(硫芥子气)	$\Delta R/R_0$:−2.09%(沙林);−3.95%(硫芥子气)	[71]
SnS_2/rGO 复合材料	化学电阻	室温	沙林、硫芥子气	0.05 mg·m^{-3}(沙林);0.1 mg·m^{-3}(硫芥子气)	95 s(沙林);47s(硫芥子气)	$\Delta R/R_0$:−3.54%(沙林);−10.2%(硫芥子气)	[72]
石墨烯(UV 激活)	FET	室温	DMMP	8.0×10^{-7} mol·mol^{-1}(UV 照射下)	—	响应增强因子(≈54 倍)[b]	[60]
非堆叠 rGo−六氟羟丙基苯(3D 多孔 rGO 共价受体)	QCM	室温	DMMP	4.0×10^{-6} ~ 1.28×10^{-4} mol·mol^{-1}	响应约 22 s、恢复约 27 s	Δf:43 ~241 Hz	[73]
多层多孔 rGO 框架	化学电阻	室温	DMMP	2.0×10^{-7} mol·mol^{-1}	—	$\Delta R/R_0=2.21\%$(10^{-6} mol·mol^{-1});$\Delta R/R_0=8.95\%$(5.0×10^{-5} mol·mol^{-1})	[74]
rGO 薄膜网络	化学电阻	室温	HCN、DMMP、2−氯乙基乙基硫醚、2,4−二硝基甲苯	约 10^{-9} mol·mol^{-1}(10 s 暴露)	—	可逆电阻响应(10^{-3} mol·mol^{-1})	[75]

注:a 响应指标根据传感平台定义:化学电阻型传感器的响应定义为相对电阻变化 $\Delta R/R_0$;FET 型传感器的响应表征为沟道电导或电流的变化;"可逆"表示在气体引入与去除过程中,传感信号可随之重复上升与恢复至初始基线水平,未观察到明显不可逆漂移;QCM 传感器的响应定义为共振频率变化 Δf。气体浓度以 mol·mol^{-1}表示;$\Delta R/R_0$ 为无量纲比值;Δf 单位为 Hz。

b 响应增强因子定义为在外界激励(如紫外照射)条件下的传感器响应与无激励条件下的响应之比。

1.2.2 应力/应变传感器

针对智能穿戴与无人平台结构健康监测的轻量化需求,二维材料是构建下一代柔性传感器的理想选择。MoS_2 因其三层原子的结构和 Mo—S 离子键而具有显著的压电效应和优异柔性,在高性能柔性场效应晶体管领域表现突出[77-78],已在4英寸(1英寸 = 2.54 cm)基底上实现密度达1 518个/cm^2的大规模集成,成功制备出反相器、静态随机存取存储器等多级集成电路[61,79],为人员状态监测与结构健康监测提供了高集成、超低功耗的解决方案。石墨烯则利用高强度、宽应变范围(293%)[80]及卷对卷等低成本工艺的兼容性,在智能织物领域极具潜力。相比之下,$Ti_3C_2T_x$ 等 MXene 材料展现出独特的多功能性:不仅具备极高的灵敏度(敏感系数高达2 369.1)[81],其碳复合泡沫更在低负载(质量分数为3%)下实现了优异的 EMI 屏蔽(>25 dB)[82],达成了"传感-防护"一体化。当前核心挑战在于平衡高灵敏度与长期稳定性,并攻克复杂工况下的器件抗氧化老化难题[82-83]。

1.2.3 光电探测器

二维材料凭借独特的宽谱响应与超快载流子迁移率,成为激光通信、夜视成像及精密制导系统的核心候选材料[62,84]。石墨烯的零带隙特性覆盖了从紫外至太赫兹的超宽波段,皮秒级响应速度完美适配高速激光通信。黑磷及其衍生物则因窄带隙和面内各向异性,成为中红外偏振探测的代表,在复杂背景目标识别方面前景广阔[62,84-86]。与之互补,新兴 TMDs(如 $PtSe_2$)具有层数依赖的可调带隙(1.2 eV 至 0 eV)及优于黑磷的环境稳定性,为长寿命中长波红外探测提供了新选择。尽管二维材料在非制冷红外成像与柔性器件方面已获突破[87],但其在高性能夜视、导引识别和中红外通信等前端的工程部署,仍受限于原子级厚度导致的光吸收效率瓶颈及异质结工艺的一致性难题[88]。未来亟须聚焦新型异质结构设计、提升光吸收效率,并突破与 CMOS 兼容的异质集成工艺。

1.2.4 医学检测

先进生物医学是二维材料发挥其表面敏感性优势的关键领域,涵盖了从临床体外诊断到可穿戴健康监测的全链条应用。

在代谢物监测与免疫诊断方面,二维材料显著提升了电化学界面的信噪比与催化活性。利用 rGO 与 MXene 的高导电性及丰富活性位点,为酶电化学传感器提升了电荷转移效率与信噪比,以实现对汗液、泪液等连续代谢物中多种生物标志物(葡萄糖、乳酸等)的无创监测,也有效克服了非酶传感器对碱性环境的依赖[89-90]。在临床血清测试中,通过共沉积层结构优化的二维免疫电极,成功实现了对乙肝(0.01 ng/mL)、梅毒及人类免疫缺陷病毒(0.11 ng/mL)等传染源的超低限度多通道筛查[91],为低成本即时检测提供了强有力的技术支撑。

在高危病原体筛查方面,FET 与微纳光学传感呈现互补优势。石墨烯 FET 凭借原子级沟道对表面电场的极高敏感度,在新型冠状病毒感染(coronavirus disease 2019,COVID-19)临床拭子检测中展现优异的瞬时响应能力,在复杂介质下检出限仍低至 100 fg/mL[63];而 MoS_2 FET 则因优异的亚阈值摆幅,实现了对链霉亲和素等蛋白分子的飞摩尔级(100 fM)响应[92]。与之呼应,基于氧化石墨烯的"磁性-表面增强拉曼散射"探针与微流控芯片,利用化学增强与电磁热点的协同作用,在无须复杂扩增的前提下,实现了对沙门氏菌及甲型 H1N1 流感病毒的超灵敏无损识别,进一步拓宽了传染病现场预警的技术路径[93-94]。

尽管前景广阔,该领域仍面临三大临床转化瓶颈:一是高离子强度体液环境中的德拜屏蔽效应限制了 FET 探测深度[95];二是复杂生理介质中的非特异性吸附导致信号漂移;三是器件封装的生物兼容性与批次间一致性仍需工程化验证。

1.3 轻量化防护与防腐

在现代高技术装备领域,防护技术的"重量-性能"倒置困境严重制约了装备的机动性与有效载荷(SWaP 限制)。传统防护材料依赖物理增厚抵御冲击,而有机防腐涂层在深海高压及高超声速气动热等极端环境下已逼近其物理化学极限。相比之下,二维材料利用其本征强化学键高效吸能,并凭借低原子质量实现减重;同时,通过延长腐蚀介质的渗透路径,结合电偶保护体系或在金属表面诱导形成致密钝化层实现高效防腐。二维材料凭借原子级厚度、超凡的比强度(强度-密度)以及独特的物理阻隔特性,既能以极低密度实现超越钢铁的承载力,又能构建不可渗透的化学屏障,成为下一代轻量化、高强韧、长效防腐体系的战略基石。

1.3.1 抗高速冲击防护

二维材料在轻质抗冲击防护方面的核心优势在于其无与伦比的比强度和独特的能量耗散机制。石墨烯单层厚度仅 3.35 Å,却拥有高达130 GPa的断裂强度和1.0 TPa 的杨氏模量,是钢

的 200 倍以上[16]。这种超高强度源于其 sp^2 杂化碳原子构成的六元环蜂窝结构,使得载荷可通过共价键网络高效分散。Thomas 等研究发现,多层石墨烯在超声速冲击下展现出非凡的能量耗散能力(如图 4(a)所示):在 600 m/s 和 900 m/s 冲击速度下,其比吸能分别达 1.26 MJ/kg 和 0.86 MJ/kg,是同等条件下钢板的 10 倍以上[96]。这种优异性能源于其受冲击时的锥形变形及沿晶向扩展的径向裂纹,能有效将点载荷转化为面内拉伸,显著提升了防护效能。

1.3.2　抗热冲击与阻燃涂层

在极端热环境防护方面,二维材料同样表现突出。h-BN 由于其强 B-N 的 sp^2 杂化和电荷转移而具有卓越的热稳定性(空气中 >850 ℃稳定)和化学惰性(1 500 ℃的极端条件下也不与大多数物质发生化学反应),成为抗热冲击涂层的首选[97-98]。Ajayan 团队首次利用化学气相沉积(chemical vapor deposition,CVD)技术制备的大面积超薄 h-BN 涂层(如图 4(b)所示),在 1 100 ℃极端氧化环境下仍能有效保护金属基底[98]。在复合材料中,h-BN 显著提升了聚合物的阻燃性能。研究表明,引入 MXene@h-BN 纳米复合物或者羟基化 h-BN 不仅能大幅提高聚二甲硅氧烷和硅橡胶的热导率,更能利用物理屏障效应阻隔热流与挥发物,使峰值热释放率降低 50% ~ 70%[99-100]。Jimenez 等的实验进一步证实,h-BN 复合涂层在 1 400 ℃火焰冲击下依然能保持内部结构完整性,并显著抑制有害气体释放[101]。

1.3.3　抗腐蚀涂层

二维材料在金属腐蚀防护领域展现出独特的“纳米屏障”与“活性防护”双重潜力。其利用高径厚比特性在涂层中构建“迷宫效应”(如图 4(c)所示),有效延长腐蚀介质的渗透路径[102-103]。其中,部分二维导电材料可通过调控界面电荷转移过程实现腐蚀抑制,例如通过构建电偶保护体系或在金属表面形成致密钝化层[103-104]。Ruoff 团队证实,CVD 石墨烯涂层可使铜箔在 200 ℃及强氧化溶液中保持表面光洁,展现出优异阻隔性[105]。Ajayan 等构建的 h-BN/聚乙烯醇复合涂层,利用疏水介电特性将氯离子渗透效率降低 98.7%,年腐蚀速率降至 1.19×10^{-3} mm[106]。此外,$Ti_3C_2T_x$ 等 MXene 材料因其独特的层状结构,仅需微量添加(1%)即可显著降低腐蚀电流并提升耐磨性,延长涂层服役寿命[107]。

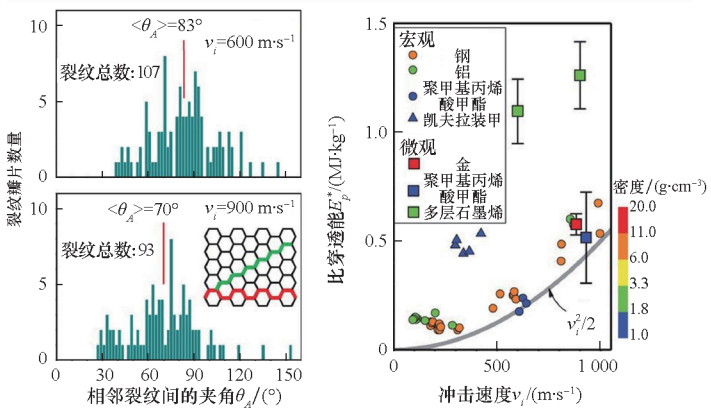

(a) 多层石墨烯抗冲击防护[96]

(a) Impact protection of multilayer graphene[96]

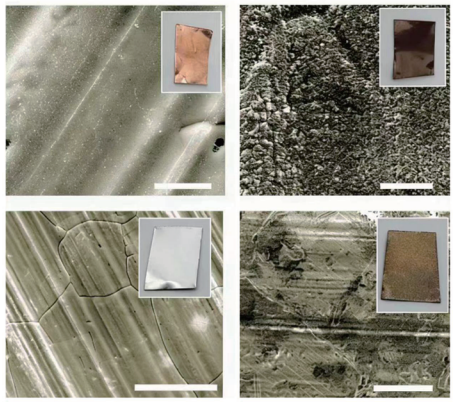

(b) h-BN 涂层高温抗氧化[98]

(b) High-temperature oxidation resistance of h-BN coatings[98]

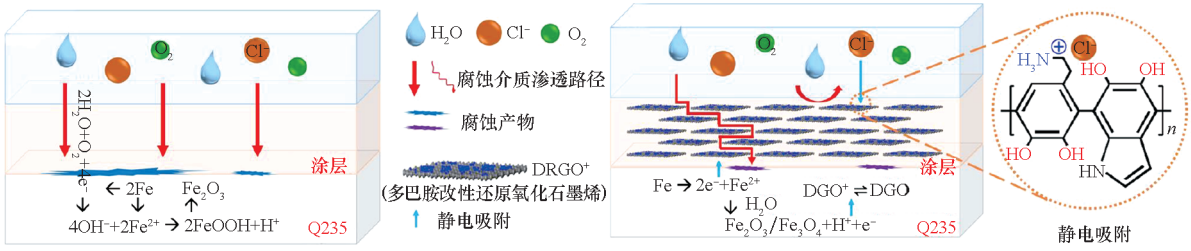

(c) 二维材料防腐机制[102]

(c) Anti-corrosion mechanisms of 2D materials[102]

图 4　二维材料有效防护和防腐

Fig. 4　Effective protection and anti-corrosion of 2D materials

二维材料为打破“防护 - 减重”悖论提供了新范式,但工程化应用仍面临挑战:一是纳米尺度分散难题,高比表面积易致团聚,成为导致应力集中的缺陷;二是界面结合强度不足,弱相互作用限制载荷传递;三是潜在的电偶腐蚀风险,导电涂层破损后可能加速基体腐蚀。未来亟须攻克表面改性与规模化组装工艺,解决可靠性难题,推动其在相关前沿技术领域的实战落地。

1.4　高效能源与动力

在智能化装备体系中,便携式系统、无人平台及高功率载荷(如电磁发射、激光器)对能源系统提出了高比能、高功率及极端环境适应性的严苛要求。二维材料凭借原子级厚度、高比表面积及优异的电子/热输运特性,为突破传统“能量 - 功率”鸿沟及热管理瓶颈提供了新范式:其利用薄层结构缩短离子路径以降低扩散势垒,提升功率密度;凭借海量位点实现电荷快充放;依托强共价键网络减弱声子散射,赋予其卓越的本征导热性能。本小节聚焦高能电池与超级电容器[108]、太阳能电池[109]、高功率激光元件[110],阐述二维材料在能源动力系统中的关键应用。

1.4.1　高能电池与超级电容器

特种装备往往需要兼顾长续航(高能量)与脉冲输出(高功率)。石墨烯体系利用高导电与高比表优势解决此矛盾[111-118]:Fe_3O_4/石墨烯混合器件兼具锂电级能量密度(147 Wh · kg^{-1})与超级电容级功率密度[119];仿血管分级孔结构设计(如图 5(a)所示)使离子扩散系数提升 14 倍,实现了高负载下的柔性固态储能[120];垂直石墨烯包裹的硅碳微米球(如图 5(b)所示)利用界面协同效应,在高面载量下实现了能量与功率密度的同步提升[121]。MXene($M_{n+1}X_nT_x$)兼具高导电性、赝电容行为与高密度优势[122-124],在紧凑型储能中表现卓越:$Ti_3C_2T_x$/RuO_2 全赝电容器件在 20 000 次循环后容量保持率达 86%[125];构筑垂直通道的 MXene/碳纳米管(carbon nanotube, CNT)电极在 - 50 ℃ 极寒环境下仍保持 10.17 Wh · kg^{-1}的能量密度(如图 5(c)所示),具备极端环境可靠性[126]。鉴于传统高熵材料在 Li-S 电池及锂电池中已展现卓越性能[127-129],若将高熵设计理念拓展至二维体系,有望实现更高能量密度与耐环境能力,支撑极限工况应用。

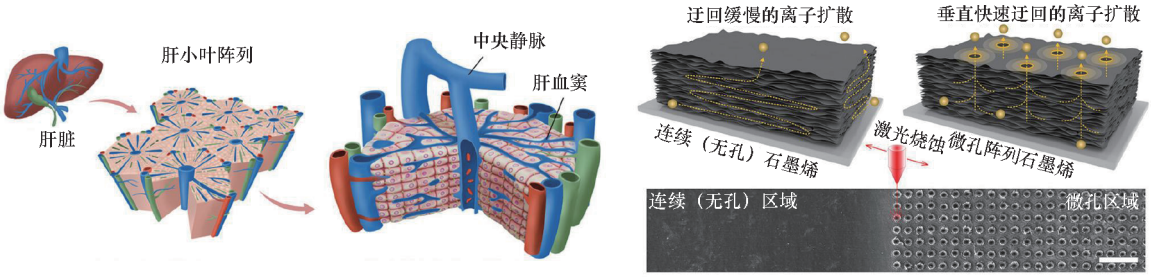

(a) 仿血管结构的石墨烯柔性固态超级电容器[120]

(a) Biomimetic vascular graphene flexible solid-state supercapacitor[120]

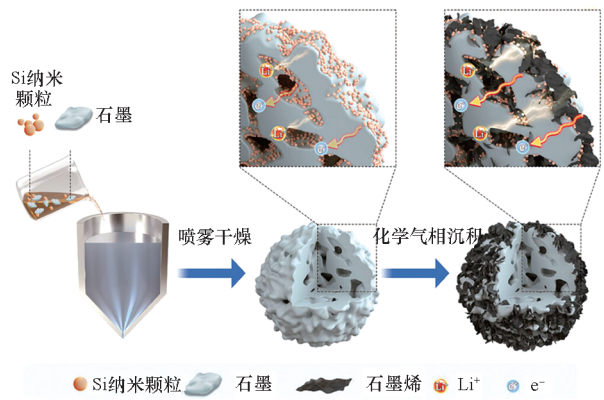

(b) 垂直石墨烯/硅碳复合微米球协同提升能量与功率密度[121]

(b) Vertical graphene/Si/C composite microspheres synergistically enhancing energy and power density[121]

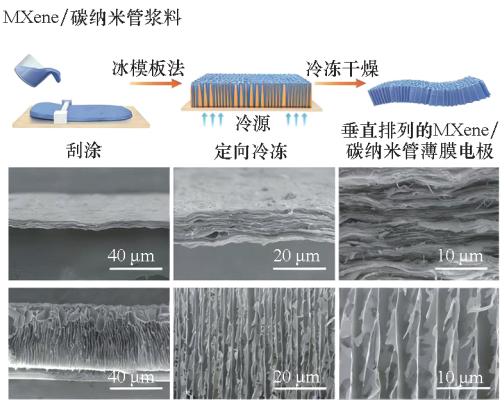

(c) 耐低温 MXene/CNT 复合电极[126]

(c) Low-temperature resistant MXene/CNT composite electrode[126]

图 5　二维材料用于电池与电容器

Fig. 5　2D materials for batteries and capacitors

1.4.2　太阳能电池

针对无人机与便携设备的长续航需求,二维材料成为提升钙钛矿光伏稳定性与效率的关键[130-132]。TMDs(如 MoS_2)平整无悬键表面可作为生长模板抑制离子迁移并优化电荷传输[133],其改性效果已被大量实验与理论工作所证实[134-147]。Zai 等利用晶圆级 MoS_2(如图 6(a)所示)封装钙钛矿,实现单电池 26% 的高效率,且在 85 ℃下运行 1 200 h 仅衰减 4%[148]。Park 等采用介孔结构 MoS_2 作为电子传输层(如图 6(b)所示),改善晶体生长,将效率提升至 25.7% 并稳定运行超过 2 000 h[149]。尽管潜力巨大,但大面积制备的均匀性与缺陷控制仍是工程化应用的主要障碍,需结合原子级模拟[150]与生长工艺优化进一步突破。

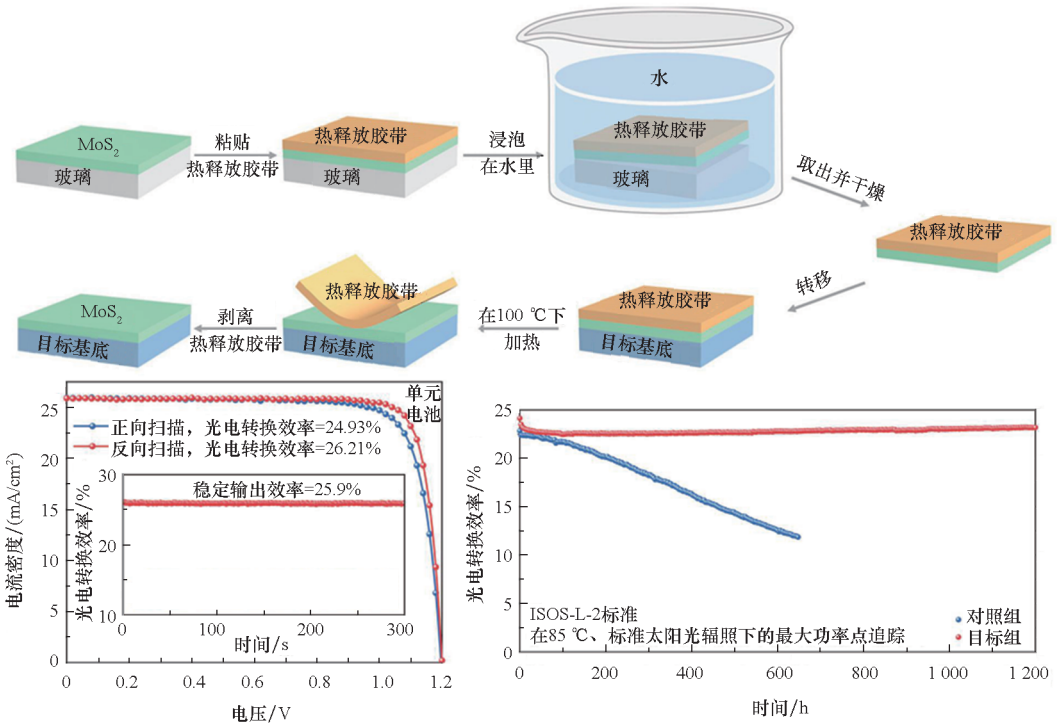

(a) 晶圆级 MoS_2 封装钙钛矿[148]

(a) Wafer-scale MoS_2 encapsulating perovskite[148]

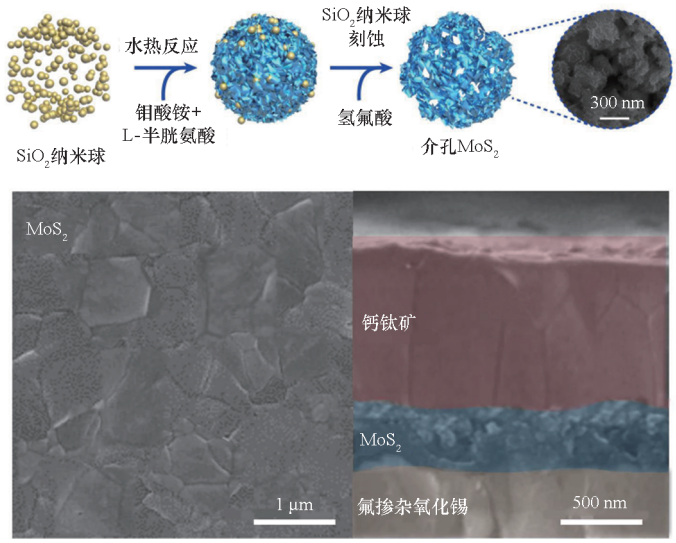

(b) 介孔 MoS_2 增强钙钛矿界面耦合[149]

(b) Mesoporous MoS_2 enhancing perovskite interfacial coupling[149]

图 6　MoS_2 用于钙钛矿太阳能电池

Fig. 6　MoS_2 for perovskite solar cells

1.4.3　高功率激光元件

热管理是高功率激光系统维持波束质量的核心。石墨烯(5 000 W/(m · K))与单层$MoSi_2N_4$(173 W/(m · K))[151]的高热导率(如图 7(a)所示)提供了高效散热路径。h-BN 兼具绝缘和高导热特性,Gu 等构建 CoNi@ h-BN/聚二甲基硅氧烷(polydimethylsiloxane, PDMS)复合薄膜(如图 7(b)~(c)所示)实现了电磁屏蔽(-49.9 dB)与散热(7.31 W/(m · K))的协同,适用于紧凑轻量化激光系统[152]。此外,人工智能(artificial intelligence,AI)辅助材料设计正加速新型高热导二维材料的发现(如图 7(d)所示),为激光元件热管理提供新思路[153]。

二维材料有力支撑了特种能源系统在"能量-功率"平衡及极限热管理上的突破。然而,迈向工程化应用仍面临关键瓶颈:一是体积性能受限,低振实密度导致体积能量密度不足,难以满足高机动平台等空间受限装备的极致需求;二是界面耦合难题,层间范德华接触引发的界面热阻削弱了散热优势;三是大面积制备一致性,难以在工业尺度上获得高可靠谱性无缺陷薄膜。未来亟须聚焦

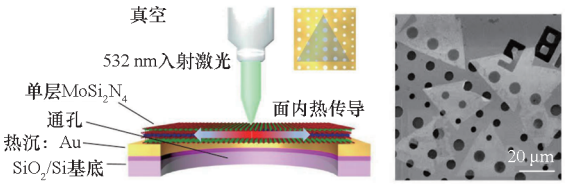

(a) 高热导率悬浮单层 $MoSi_2N_4$[151]

(a) High thermal conductivity suspended monolayer $MoSi_2N_4$[151]

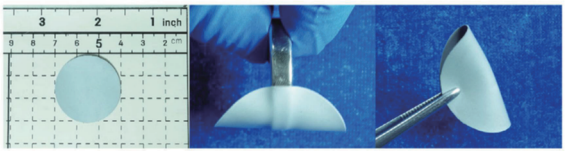

(b) 二维复合柔性材料[152]

(b) Flexible 2D composite materials[152]

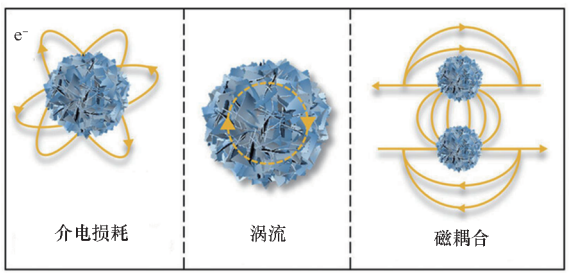

(c) 二维复合柔性材料用于电磁屏蔽和散热[152]

(c) Flexible 2D composite materials for electromagnetic shielding and heat dissipation[152]

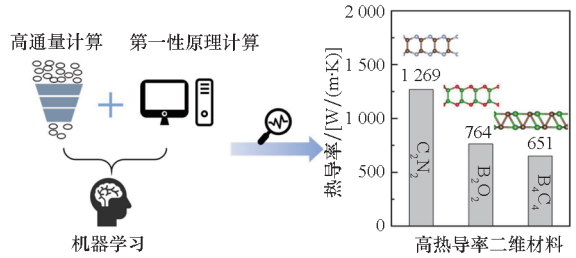

(d) 机器学习辅助预测高热导率材料[153]

(d) Machine learning assisted prediction of high thermal conductivity materials[153]

图 7　二维材料热管理应用

Fig. 7　2D materials for thermal management applications

致密化电极设计、原子级界面焊接及晶圆级生长工艺,以跨越从材料特性到系统效能的工程鸿沟。

1.5　量子技术与信息安全

量子技术通过操控微观粒子量子态(如叠加、纠缠),正推动通信、计算与传感领域的变革与计算范式的重构,而二维材料独特的原子限域效应与理化调控机制为其提供了理想实现方案。二维材料利用禁带缺陷引发的量子限域效应实现确定性单光子发射,为量子加密提供安全光源;通过电场驱动下的离子迁移或相变机制实现电导连续调制,模拟神经突触行为;凭借极高的载流子迁移率与本征自旋特性,突破高频响应极限。本节聚焦量子通信加密、神经形态计算及高频电子通信,阐述二维材料在提升信息安全与处理能力方面的关键作用。

1.5.1　量子通信加密

面对传统加密算法可能被未来量子计算机破解的威胁,基于量子力学原理的保密通信成为必然选择。二维材料中的固态单光子源,是构建量子密钥分发等协议中不可克隆的"理想光源"的关键。二维材料独特的原子层状结构赋予其强激子束缚能、宽光谱可调性与优异外场响应等本征物理特性,进而转化为单光子源在微型化、集成化与可控性上的突出应用优势。其体系主要分为两类:一是基于二维半导体(如 WSe_2、$MoTe_2$)[154-156]或 h-BN[157]中本征/人工缺陷的"量子点"[154-157]单光子源,它们通过局域载流子实现稳定、窄线宽的发射(如图 8(a)所示);二是利用单层二维材料中受限激子[158-162]本身作为发射单元(如图 8(b)所示),这类源具有天然的原子级厚度和强大的光-物质相互作用,且其发射特性可通过外加电场、磁场或机械应变进行灵活调控[163-165],为集成化量子光源的设计提供了便利。为满足实用化对光源亮度、稳定性及与通

信波段(如光纤低损耗窗口)匹配的苛刻要求,研究者们发展了基于对称性破缺的缺陷工程、利用拓扑位错作为鲁棒性发射中心等新策略[166-168]。迈向大规模应用的核心挑战在于实现单光子发射位点的确定性、可寻址制备,并与片上波导等光子元件高效集成,这正是当前外场工程与范德华异质结技术重点攻关的方向。

1.5.2　神经形态计算

传统冯·诺依曼架构面临功耗与效率瓶颈[2],难以适配海量数据的实时处理需求。类脑芯片通过忆阻器模拟突触权重,有望突破这一架构限制。二维材料凭借原子级厚度的层状结构及丰富的光电特性,为构筑高性能纳米忆阻器奠定了基础[169-171]。其原子级超薄结构带来的界面可控性、载流子输运特异性与环境稳定性等物理特性,直接转化为忆阻器低功耗、高耐久、易集成与极端环境适配的应用优势。

二维材料忆阻器开关机制主要涵盖经典型[172-175]与量子型[176-180]两类:经典效应上,MoS_2[172]可通过电场调控 Li^+ 迁移,实现相态可逆转变,进而调节开关状态并模拟突触功能(如图 8(c)所示);量子效应方面,石墨烯/$MoS_{2-x}O_x$/石墨烯异质结忆阻器[180]可耐受 340 ℃高温、超 10^3 次弯曲及 10^7 次开关,为航空航天等恶劣环境下的器件应用提供了新方案(如图 8(d)所示)。尽管潜力巨大,该领域仍需攻克单光子精确定位、极端条件下结构稳定性及量子态精准调控等难题,未来亟须聚焦于提升系统的抗干扰能力与调控精度。

1.5.3　高频电子通信

在雷达、卫星通信等高频前端系统中,对器件的噪声、线性度、功率及抗干扰能力有极高要求。单层/少层蛭石兼具宽带隙与反铁磁(antiferromagnetic,AFM)基态,且易于规模化制备[181-182],契合高性能高频链路对高击穿、低漏电及频谱稳定性的需求。二维蛭石的天然原子层状层叠结构,赋予其宽带隙、AFM 基态与高制备兼容性的优异物理特性,进而转化为高频应用中低噪声、高击穿、强抗干扰与易片上集成的核心应用优势。AFM 无净磁矩、抗磁干扰且具备 THz 级自旋振荡特性[183](如图 8(e)所示),是进入高频前端的关键。二维蛭石不仅能作为低噪声源,还能与 h-BN 等构建范德华异质结实现片上互补。此外,针对空间/特种场景的抗辐射要求,MoS_2 等材料在特定粒子辐照下表现出的缺陷自愈特性[184-185](如图 8(f)所示),为二维高频器件在“耐辐照-噪声谱-带宽”间的平衡设计提供了依据。

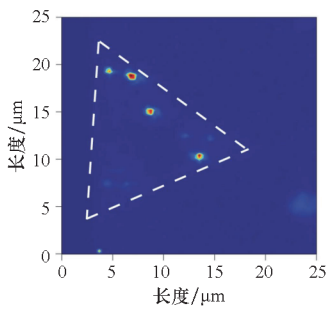

(a) 单层 WSe_2 中单光子源的光致发光光谱[154]

(a) Photoluminescence spectrum of single-photon source in monolayer WSe_2[154]

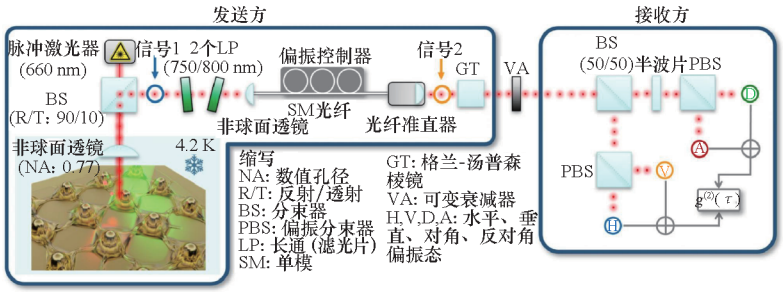

(b) 基于单层 WSe_2 的 BB84-QKD 架构[158]

(b) BB84-QKD architecture based on monolayer WSe_2[158]

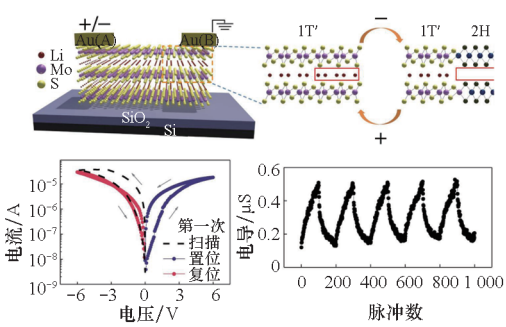

(c) Au/MoS_2/Au 忆阻器结构、原理以及电导特性[172]

(c) Structure, mechanism and conductance characteristics of Au/MoS_2/Au memristor[172]

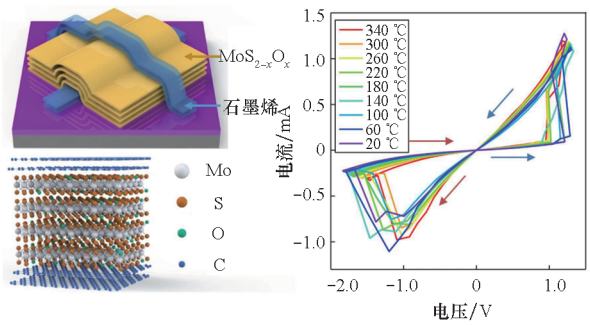

(d) $MoS_{2-x}O_x$/石墨烯异质结的器件示意图及开关特性[180]

(d) Schematic and switching characteristics of $MoS_{2-x}O_x$/graphene heterojunction device[180]

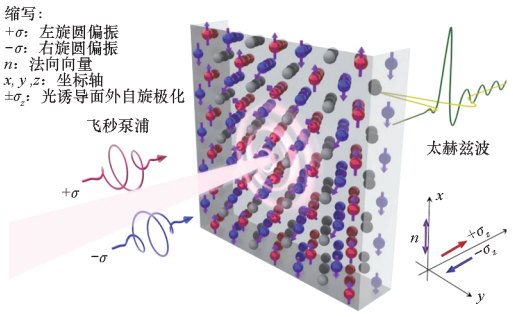

（e）Mn_2Au 中的太赫兹自旋振荡[183]

（e）Terahertz spin oscillation in Mn_2Au[183]

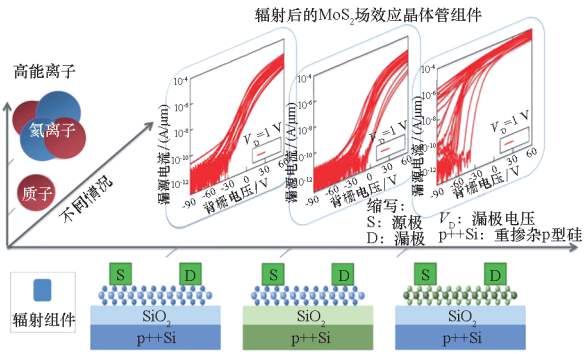

（f）原子级薄 MoS_2 器件的抗辐射性能[185]

（f）Radiation hardness of atomically thin MoS_2 device[185]

图 8　量子技术与信息安全

Fig. 8　Quantum technology and information security

2　面临的挑战

尽管二维材料在实验室中展现出颠覆性潜力，但其迈向规模化、高可靠性的工程应用仍需跨越三大核心挑战：规模化制备、环境稳定性与技术标准化。

2.1　规模化制备

2.1.1　晶圆级生长

当前研究正经历从“样品级可控”到“晶圆级均匀”的关键转型[186]，且不同材料体系的核心制备壁垒与工艺策略存在着显著差异。

石墨烯的生长难点主要在于消除多畴晶界缺陷及转移过程中的污染。利用 Cu(111)单晶缓冲层技术，目前已实现晶圆级单晶石墨烯的无缝拼接与无损制备，有效抑制了多晶散射[187]；欧盟 2D-EPL 计划的多项目晶圆流片显示器件良率超 85%，进一步验证了其与标准化工艺流的兼容性[188]。相比之下，化合物半导体（如 TMDs 与 InSe）的制备更依赖于前驱体动力学与热预算的精准调控。针对 InSe 的相纯度难题，通过抑制多相竞争与精确调节化学计量比，已成功获得晶圆级纯相薄膜[189]。对于 MoS_2，改进的 CVD/金属有机化合物气相沉积（metal-organic chemical vapor deposition，MOCVD）技术已实现 12 英寸单层均匀生长[190-191]；为解决 CMOS 热兼容性与晶畴取向问题，低温 MOCVD 与衬底台阶边缘诱导成核策略被相继开发，在满足硅基后道工艺热限制的同时消除了旋转畴缺陷，使器件良率突破 94%[192]。此外，MXene 的规模化制备则面临截然不同的液相挑战，主要集中在刻蚀均一性与表面官能团的精准调控。

尽管进展显著，产业化应用仍受限于三大瓶颈：一是缺陷控制，现有工艺难以完全避免原子级空位，亟须精细化的掺杂与修复策略；二是工艺整合，学术界报道的高良率往往局限于特定衬底，向商业化 CMOS 产线转移时仍面临光刻胶残留与封装裂纹等工程难题；三是合成安全，替代剧毒前驱体的绿色合成路径是高性能 TMDs 走出实验室的先决条件。

2.1.2　量产集成

量产集成的核心挑战是实现与 CMOS 兼容的低损伤金属接触。传统沉积易引发损伤与费米能级钉扎，限制器件性能。为此，研究者开发了利用半金属铋、预制电极转移及 CVD 生长金属电极等范德华接触策略，实现了近零势垒欧姆接触[193-195]。目前该工艺已在 4 英寸晶圆上集成超 2.5 万个单元，接触电阻降至 5.3 kΩ · μm[196]。尽管此类创新提升了肖特基结性能，但仍需进一步解决大面积可控性、CMOS 兼容性以及半金属接触的长期可靠性问题。

2.2　环境稳定性

黑磷、TMDs、硅烯等材料易受环境氧化，严重威胁器件可靠性[197]。特别是硅烯、硼烯等单质材料，由于存在大量不饱和键与亚稳态结构，其稳定性极差，通常仅能存在于超高真空环境中。针对此类材料，目前必须依赖生长后的原位封装（如覆盖非晶层或构建范德华异质结）进行隔绝，这种严苛的真空与加工限制极大地增加了器件制备与转移的难度，成为其应用拓展的主要瓶颈。

对于黑磷等相对稳定的材料，现有防护策略主要采用 h-BN 封装或原子层沉积技术构建物理屏障，以及进行表面化学修饰[198]。然而，上述手

段效果有限,且工艺过程中的褶皱与污染进一步削弱了器件一致性[199]。尽管石蜡辅助转移与机械平整等工艺改善了材料的结构完整性,但在高湿、强辐照及温差骤变等极端工况下仍显乏力[200]。鉴于先进装备需在复杂工况下长期稳定运行,攻克环境稳定性瓶颈是二维材料迈向工程化应用的必经之路。

2.3　技术标准化

为确保二维材料在特种装备中实现可复制、可审计的长期可靠性,关键在于构建涵盖“术语计量—材料准入—工艺与堆叠—器件鉴定—环境与 EMC—空间与辐照”的工程闭环标准体系。

第一,术语与计量的统一。以 GB/T 30544.13—2018(等同 ISO/TS 80004 - 13)统一层数、缺陷等口径;以涵盖拉曼光谱(Raman spectroscopy, Raman)、X 射线衍射(X-ray diffraction,XRD)、透射电子显微镜(transmission electron microscopy,TEM)等的 T/CSTM 00166 系列统一表征方法;以 T/CGIA 002—2018 约束命名与披露。项目层面强制留存“样品 ID—制备路径—层数/厚度—缺陷密度—离子/水含量—标准化谱图(Raman/XRD/TEM)—解析口径”,并写入质量记录与审计清单[201 - 203]。

第二,材料/中间体分级与真空洁净准入。针对薄膜、粉体/浆料、转移膜、复合层等供货形态,纳入 QJ 1558B—2016 做准入与来料抽检,以总质量损失/收集的可凝挥发物/水汽回吸量,筛除高逸出风险,抑制光学载荷与射频前端漂移;对蛭石的层间水合、阳离子残留实施批次监测与留样追溯[204]。

第三,转移/封装/异质结堆叠过程控制。以 T/CSTM 00166 为锚点,设定界面有机残留、金属杂质、溶剂足迹阈值与去残留流程;将“扭角容差—性能漂移”测量纳入检验;空间应用在工艺冻结前完成 QJ 1558B—2016 出气筛选与热真空预处理[202 - 204]。

第四,器件级鉴定以特种标准为基准。依托 GJB 548C—2021 与 GJB 360B—2009,覆盖温度/湿热、循环/冲击、振动、加速寿命等;把阈值电压、跨导、1/f 噪声、相位噪声、起振门限等固化到“指标—失效判据—样本量—统计方法”的器件规范与数据审计清单[205 - 206]。

第五,环境试验与可变形载荷叠加。系统层面按 GJB 150.1A—2009,元器件层面按 GB/T 2423 系列;在温湿振/冲击中叠加弯折/拉伸循环与在线电/光/自旋监测,建立“机械循环—性能衰减—失效模式”统计关联,支撑寿命模型与冗余[207 - 208]。

第六,EMC 与系统准入。系统级执行 GJB 151B—2013,按传导发射—传导抗扰度—辐射发射—辐射抗扰度闭环验收;材料侧筛选可用团体/企业标准,但以 GJB 151B—2013 限值与边界判定;片上高频模块重点观测相位噪声、寄生辐射与耦合路径[209]。

第七,空间与强辐照三位一体评估。辐射谱按 GJB/Z 24—1991 与 GJB/Z 24A—2020 建模并合成地面谱;单粒子效应按 GJB 7242—2011 与 QJ 10005—2008 开展单粒子翻转/单粒子锁定并评估线能量传输与截面;材料/涂层按 GJB 2502 系列(如 GJB 2502.6—2006)评估真空 - 质子辐照。相关文献指出该体系已在地面模拟与在轨验证中广泛采用并持续完善[210 - 214]。至此,从材料到标准的纵向通道与横向场景实现了方法学层面的统一。

3　发展趋势

面对特种装备向智能化、微型化及多功能一体化演进的需求,基于二维材料的前沿技术正从“单一性能突破”逐步走向“系统级协同创新”。单纯依赖材料本征特性的优化已难以满足未来复杂工况下对装备 SWaP 指标与任务适应性的极致追求。未来发展应沿“材料层—结构层—系统层—协同层”层级递进展开,如图 9 所示。

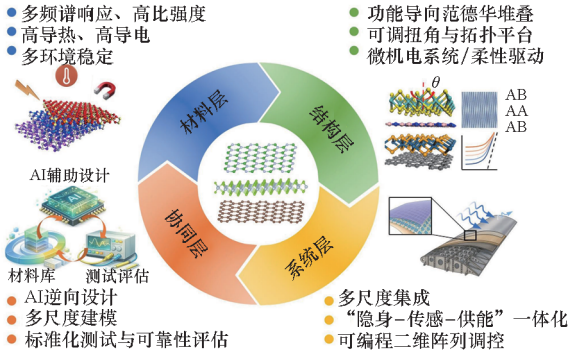

图 9　二维材料前沿技术领域展望

Fig. 9　Outlook of 2D materials in frontier technology fields

3.1　材料层:多物理场协同的智能材料

发展具备可编程与记忆特性的智能响应材料,是实现装备自适应感知与动态调控的基础。未来研究应聚焦于离子铁电、相变及电荷有序等新型物态,系统揭示其在电、光、力等多物理场诱导下的物性演化规律,并在提升环境稳定性和循

环寿命的同时,兼顾响应速度、调制精度、能耗与硅基 CMOS 工艺的兼容性,为大规模阵列化应用提供关键的功能基元。

3.2 结构层:异质集成与堆叠工程

范德华堆叠、转角电子学与三维异质集成为二维材料赋予了全新的结构调控自由度。通过在原子尺度下对层序、扭转角及层间距的精准操控可在垂直体系中构筑莫尔超晶格、强光 - 物质耦合界面及拓扑能带,实现宽带吸收、频谱整形与非线性增强。结合应变工程或微机电系统技术,可实现芯片或曲面基体上功能的动态调制,推动二维材料从单一薄膜向多尺度、层级化功能结构的演进,为系统集成奠定器件基础。

3.3 系统层:多功能集成与体系化应用

二维材料的价值正从提升单项指标转向增强装备一体化能力。集成应用可分三个维度展开:芯片级,构建兼具感知、存储与本地计算能力的"感 - 存 - 算"一体化节点;组件级,将二维材料与散热、电源、天线结构协同设计,实现电磁、热与能量流的联合调控;平台级,在飞行器蒙皮等外覆层构建大面积功能网络,实时调制局域电磁与辐射特性,实现雷达/红外特征综合管控与任务自适应重构。

3.4 协同层:AI 驱动设计与标准体系

人工智能、数字孪生与标准体系将贯穿二维材料研发的全生命周期。一方面,利用机器学习与多尺度建模在海量数据中快速筛选候选体系,建立从任务需求到材料工艺的逆向映射,实现跨尺度协同设计。另一方面,需完善参数计量、环境可靠性评估及任务谱验证规范,构建可复现、可审计的数字化验证框架。通过 AI 驱动设计与标准体系的协同约束,将加速二维材料从实验室样品向特种装备实战应用的转化。

4 总结

综上所述,二维材料凭借其原子级厚度、量子限域效应、优异的力热光电特性及超高比强度等独特优势,已成为发展前沿技术的重要载体。本文系统综述了其在隐身与电磁屏蔽、传感与探测、轻量化防护与防腐、能源与动力、量子技术与信息安全五大核心领域的最新进展,深刻阐述了其在多频段一体化隐身、实时环境态势感知、恶劣工况长期服役防护、极端能量存储与转换及未来量子信息处理等场景中的应用价值。尽管实验室层面的原理验证已展示出颠覆性潜力,但二维材料要真正实现从"样品"向"产品"、从"实验室"向"工程化"的跨越,当前仍然面临着三大挑战:①低成本规模化制备;②极端环境下的稳定性与可靠性;③标准化检测与统一评价体系。最后,本文展望了二维材料在前沿技术领域的未来发展方向:①体系筛选与机理深究,筛选具备多维度优异性能的材料体系,并深入探究其本征服役性能与失效机制;②工艺革新与结构优化,开发绿色、低成本、高通量的晶圆级制备工艺,提升材料结构稳定性及其与微电子工艺的兼容能力;③交叉融合与智能设计,将理论与实验相结合,探究新的异质结构设计、转角电子学、应变工程及与 AI/量子计算的交叉融合机制。

参考文献(References)

[1] TRAN D C, PHAM G H, HUONG CHU T T, et al. Layer-by-layer growth of two-dimensional tellurium thin films via ultrahigh-pressure atomic layer deposition for p-type semiconductors[J]. Nano Letters, 2024, 24(51): 16276 - 16282.

[2] LIU C S, CHEN H W, WANG S Y, et al. Two-dimensional materials for next-generation computing technologies [J]. Nature Nanotechnology, 2020, 15(7): 545 - 557.

[3] ZHAO Y D, XIE Y Z, LIU Z K, et al. Two-dimensional material membranes: an emerging platform for controllable mass transport applications [J]. Small, 2014, 10(22): 4521 - 4542.

[4] XIA F N, WANG H, XIAO D, et al. Two-dimensional material nanophotonics[J]. Nature Photonics, 2014, 8(12): 899 - 907.

[5] KIM G, HUET B, STEVENS C E, et al. Confinement of excited states in two-dimensional, in-plane, quantum heterostructures[J]. Nature Communications, 2024, 15(1): 6361.

[6] EDVINSSON T. Optical quantum confinement and photocatalytic properties in two-, one- and zero-dimensional nanostructures [J]. Royal Society Open Science, 2018, 5(9): 180387.

[7] ZHANG P K, XUE M M, CHEN C F, et al. Mechanism regulating self-intercalation in layered materials [J]. Nano Letters, 2023, 23(8): 3623 - 3629.

[8] SPLENDIANI A, SUN L, ZHANG Y B, et al. Emerging photoluminescence in monolayer MoS_2 [J]. Nano Letters, 2010, 10(4): 1271 - 1275.

[9] LU C P, LI G H, MAO J H, et al. Bandgap, mid-gap states, and gating effects in MoS_2[J]. Nano Letters, 2014, 14(8): 4628 - 4633.

[10] LONG M Q, TANG L, WANG D, et al. Theoretical predictions of size-dependent carrier mobility and polarity in graphene[J]. Journal of the American Chemical Society, 2009, 131(49): 17728 - 17729.

[11] NACLERIO A E, KIDAMBI P R. A review of scalable hexagonal boron nitride (h-BN) synthesis for present and future applications[J]. Advanced Materials, 2023, 35(6): 2207374.

[12] GUERRA V, WAN C Y, MCNALLY T. Thermal conductivity

of 2D nano-structured boron nitride (BN) and its composites with polymers[J]. Progress in Materials Science, 2019, 100: 170 – 186.

[13] ZHANG K L, FENG Y L, WANG F, et al. Two dimensional hexagonal boron nitride (2D-hBN): synthesis, properties and applications[J]. Journal of Materials Chemistry C, 2017, 5(46): 11992 – 12022.

[14] ZHANG F Y, CHENG X K, YIN Z Y, et al. Crystal-symmetry-paired spin-valley locking in a layered room-temperature metallic altermagnet candidate [J]. Nature Physics, 2025, 21(5): 760 – 767.

[15] SHARMA B K, AHN J H. Graphene based field effect transistors: efforts made towards flexible electronics[J]. Solid State Electronics, 2013, 89: 177 – 188.

[16] SUN Y W, PAPAGEORGIOU D G, HUMPHREYS C J, et al. Mechanical properties of graphene [J]. Applied Physics Reviews, 2021, 8(2): 021310.

[17] ZHANG Z H, PENEV E S, YAKOBSON B I. Polyphony in B flat[J]. Nature Chemistry, 2016, 8(6): 525 – 527.

[18] WANG Z Q, CAI G F, XIA Y X, et al. Highly conductive graphene fiber textile for electromagnetic interference shielding[J]. Carbon, 2024, 222: 118996.

[19] HUANG B, CLARK G, NAVARRO-MORATALLA E, et al. Layer-dependent ferromagnetism in a van der Waals crystal down to the monolayer limit[J]. Nature, 2017, 546(7657): 270 – 273.

[20] ZHANG W B, QU Q, ZHU P, et al. Robust intrinsic ferromagnetism and half semiconductivity in stable two-dimensional single-layer chromium trihalides[J]. Journal of Materials Chemistry C, 2015, 3(48): 12457 – 12468.

[21] RAZAQ A, BIBI F, ZHENG X X, et al. Review on graphene-, graphene oxide-, reduced graphene oxide-based flexible composites: from fabrication to applications [J]. Materials, 2022, 15(3): 1012.

[22] BASAK K, GHOSH M, CHOWDHURY S, et al. Theoretical studies on electronic, magnetic and optical properties of two dimensional transition metal trihalides [J]. Journal of Physics: Condensed Matter, 2023, 35(23): 233001.

[23] GAO Y, ZHAO L J. Review on recent advances in nanostructured transition-metal-sulfide-based electrode materials for cathode materials of asymmetric supercapacitors [J]. Chemical Engineering Journal, 2022, 430(Part 2): 132745.

[24] ASHOK KUMAR S S, BASHIR S, RAMESH K, et al. A review on graphene and its derivatives as the forerunner of the two-dimensional material family for the future[J]. Journal of Materials Science, 2022, 57(26): 12236 – 12278.

[25] HOU Z L, GAO X S, ZHANG J Y, et al. A perspective on impedance matching and resonance absorption mechanism for electromagnetic wave absorbing[J]. Carbon, 2024, 222: 118935.

[26] MENG H, WEN J H, ZHAO H G, et al. Optimization of locally resonant acoustic metamaterials on underwater sound absorption characteristics [J]. Journal of Sound and Vibration, 2012, 331(20): 4406 – 4416.

[27] HAN Y, LIU Y X, HAN L, et al. High-performance hierarchical graphene/metal-mesh film for optically transparent electromagnetic interference shielding [J]. Carbon, 2017, 115: 34 – 42.

[28] IQBAL A, HASSAN T, GAO Z G, et al. MXene-incorporated 1D/2D nano-carbons for electromagnetic shielding: a review[J]. Carbon, 2023, 203: 542 – 560.

[29] LI X L, YIN X W, LIANG S, et al. 2D carbide MXene Ti_2CT_X as a novel high-performance electromagnetic interference shielding material [J]. Carbon, 2019, 146: 210 – 217.

[30] LI Q G, ZHANG J, LIU L H, et al. Graphene-based optically transparent metasurface for microwave and terahertz cross-band stealth utilizing multiple stealth strategies [J]. Carbon, 2024, 219: 118833.

[31] LI Y, XIONG C, HUANG H, et al. 2D $Ti_3C_2T_x$ MXenes: visible black but infrared white materials [J]. Advanced Materials, 2021, 33(41): 2103054.

[32] LI X L, LI M H, LI X, et al. Low infrared emissivity and strong stealth of Ti-based MXenes [J]. Research, 2022, 2022: 9892628.

[33] LI Y, XU F, LIN Z S, et al. Electrically and thermally conductive underwater acoustically absorptive graphene/rubber nanocomposites for multifunctional applications [J]. Nanoscale, 2017, 9(38): 14476 – 14485.

[34] LIANG J J, WANG Y, HUANG Y, et al. Electromagnetic interference shielding of graphene/epoxy composites [J]. Carbon, 2009, 47(3): 922 – 925.

[35] WANG C, HAN X J, XU P, et al. The electromagnetic property of chemically reduced graphene oxide and its application as microwave absorbing material [J]. Applied Physics Letters, 2011, 98(7): 072906.

[36] HONG S K, KIM K Y, KIM T Y, et al. Electromagnetic interference shielding effectiveness of monolayer graphene[J]. Nanotechnology, 2012, 23(45): 455704.

[37] LU Z G, MA L M, TAN J B, et al. Transparent multi-layer graphene/polyethylene terephthalate structures with excellent microwave absorption and electromagnetic interference shielding performance [J]. Nanoscale, 2016, 8 (37): 16684 – 16693.

[38] ZHANG Z X, ZHOU M, ZHANG T H, et al. Few-layer borophene prepared by mechanical resonance and its application in terahertz shielding[J]. ACS Applied Materials & Interfaces, 2020, 12(17): 19746 – 19754.

[39] ZHANG Z X, YANG M Y, ZHANG Y B, et al. Research and application of terahertz response mechanism of few-layer borophene[J]. Nanomaterials, 2022, 12(15): 2702.

[40] LIN H J, WANG X M, ZHU H J, et al. Harmonizing material quantity and terahertz wave interference shielding efficiency with metallic borophene nanosheets [J]. Nature Communications, 2025, 16(1): 5739.

[41] FU Y F. Synergism of carbon nanotubes and graphene nanoplates in improving underwater sound absorption stability under high pressure [J]. Chemistry Select, 2022, 7(2): e202103222.

[42] HAN M K, YIN X W, WU H, et al. Ti_3C_2 MXenes with modified surface for high-performance electromagnetic absorption and shielding in the X-band [J]. ACS Applied Materials & Interfaces, 2016, 8(32): 21011 – 21019.

[43] THONGRATTANASIRI S, KOPPENS F H L, GARCÍA DE ABAJO F J. Complete optical absorption in periodically patterned graphene [J]. Physical Review Letters, 2012, 108(4): 047401.

[44] AMIN M, FARHAT M, BAĞCI H. An ultra-broadband multilayered graphene absorber[J]. Optics Express, 2013, 21(24): 29938 – 29948.

[45] PANWAR R, PUTHUCHERI S, SINGH D, et al. Design of ferrite-graphene-based thin broadband radar wave absorber for stealth application[J]. IEEE Transactions on Magnetics, 2015, 51(11): 2802804.

[46] YIN L X, TIAN X Y, SHANG Z T, et al. Ultra-broadband metamaterial absorber with graphene composites fabricated by 3D printing[J]. Materials Letters, 2019, 239: 132 – 135.

[47] GENG M Y, LIU Z G, WU W J, et al. A dynamically tunable microwave absorber based on graphene[J]. IEEE Transactions on Antennas and Propagation, 2020, 68(6): 4706 – 4713.

[48] ZHANG J, WEI X Z, PREMARATNE M, et al. Experimental demonstration of an electrically tunable broadband coherent perfect absorber based on a graphene-electrolyte-graphene sandwich structure[J]. Photonics Research, 2019, 7(8): 868 – 874.

[49] KIM S, JANG M S, BRAR V W, et al. Electronically tunable perfect absorption in graphene[J]. Nano Letters, 2018, 18(2): 971 – 979.

[50] YANG K X, FAN B X, YANG Y J, et al. Defect-steering the prominent thermal conduction, microwave absorption, and electrical insulation of porous g-C_3N_4 nanofibers[J]. Carbon, 2024, 219: 118849.

[51] AKA C, AKGÖL O, KARAASLAN M, et al. Broadband electromagnetic wave absorbing via PANI coated Fe_3O_4 decorated MoS_2 hybrid nanocomposite[J]. Journal of Alloys and Compounds, 2023, 967: 171702.

[52] REN H D, WANG S, ZHANG X M, et al. Broadband electromagnetic absorption of $Ti_3C_2T_x$ MXene/WS_2 composite via constructing two-dimensional heterostructure[J]. Journal of the American Ceramic Society, 2021, 104(11): 5537 – 5546.

[53] LI L, SHI M K, LIU X Y, et al. Ultrathin titanium carbide (MXene) films for high-temperature thermal camouflage[J]. Advanced Functional Materials, 2021, 31(35): 2101381.

[54] HU R, XI W, LIU Y D, et al. Thermal camouflaging metamaterials[J]. Materials Today, 2021, 45: 120 – 141.

[55] WU W, TONG L P, ZHOU H, et al. Combined experimental and DFT study on 2D $MoSe_2$ toward low infrared emissivity[J]. Advanced Functional Materials, 2022, 32(28): 2201906.

[56] YUAN B H, JIANG W K, JIANG H, et al. Underwater acoustic properties of graphene nanoplatelet-modified rubber[J]. Journal of Reinforced Plastics and Composites, 2018, 37(9): 609 – 616.

[57] LU B, LV L X, YANG H S, et al. High performance broadband acoustic absorption and sound sensing of a bubbled graphene monolith[J]. Journal of Materials Chemistry A, 2019, 7(18): 11423 – 11429.

[58] NINE M J, AYUB M, ZANDER A C, et al. Graphene oxide-based lamella network for enhanced sound absorption[J]. Advanced Functional Materials, 2017, 27(46): 1703820.

[59] LI Z L, YANG H S, LUPI S, et al. Custom-built graphene acoustic-absorbing aerogel for audio signal recognition[J]. Advanced Materials Interfaces, 2021, 8(16): 2100227.

[60] ALZATE-CARVAJAL N, PARK J, PYKAL M, et al. Graphene field effect transistors: a sensitive platform for detecting sarin[J]. ACS Applied Materials & Interfaces, 2021, 13(51): 61751 – 61757.

[61] TANG J, WANG Q Q, TIAN J P, et al. Low power flexible monolayer MoS_2 integrated circuits[J]. Nature Communications, 2023, 14(1): 3633.

[62] WU J F, ZHANG J L, JIANG R Q, et al. High-sensitivity, high-speed, broadband mid-infrared photodetector enabled by a van der Waals heterostructure with a vertical transport channel[J]. Nature Communications, 2025, 16(1): 564.

[63] SEO G, LEE G, KIM M J, et al. Rapid detection of COVID-19 causative virus (SARS-CoV-2) in human nasopharyngeal swab specimens using field-effect transistor-based biosensor[J]. ACS Nano, 2020, 14(4): 5135 – 5142.

[64] GANESAN K, RAZA S K, VIJAYARAGHAVAN R. Chemical warfare agents[J]. Journal of Pharmacy and Bioallied Sciences, 2010, 2(3): 166 – 178.

[65] CHAUHAN S, CHAUHAN S, D'CRUZ R, et al. Chemical warfare agents[J]. Environmental Toxicology and Pharmacology, 2008, 26(2): 113 – 122.

[66] DONARELLI M, OTTAVIANO L. 2D materials for gas sensing applications: a review on graphene oxide, MoS_2, WS_2 and phosphorene[J]. Sensors, 2018, 18(11): 3638.

[67] PAGHI A, MARIANI S, BARILLARO G. 1D and 2D field effect transistors in gas sensing: a comprehensive review[J]. Small, 2023, 19(15): 2206100.

[68] PERKINS F K, FRIEDMAN A L, COBAS E, et al. Chemical vapor sensing with monolayer MoS_2[J]. Nano Letters, 2013, 13(2): 668 – 673.

[69] LI B L, CHEN X W, SU C, et al. Enhanced dimethyl methylphosphonate detection based on two-dimensional WSe_2 nanosheets at room temperature[J]. Analyst, 2021, 145(24): 8059 – 8067.

[70] ALEV O, ÖZDEMIR O, GOLDENBERG E, et al. WS_2 thin film based quartz crystal microbalance gas sensor for dimethyl methylphosphonate detection at room temperature[J]. Thin Solid Films, 2022, 745: 139097.

[71] JIANG H N, WANG H Z, SHANGGUAN Y L, et al. Homogeneously niobium-doped MoS_2 for rapid and high-sensitive detection of typical chemical warfare agents[J]. Frontiers in Chemistry, 2022, 10: 1011471.

[72] LIANG T, WANG H Z, JIANG H N, et al. Highly sensitive SnS_2/rGO-based gas sensor for detecting chemical warfare agents at room temperature: a theoretical study based on first-principles calculations[J]. Crystals, 2024, 14(12): 1008.

[73] HWANG H M, HWANG E, KIM D, et al. Mesoporous non-stacked graphene-receptor sensor for detecting nerve agents[J]. Scientific Reports, 2016, 6: 33299.

[74] WANG Y Y, YANG M, LIU W X, et al. Gas sensors based on assembled porous graphene multilayer frameworks for DMMP detection[J]. Journal of Materials Chemistry C, 2019, 7(30): 9248 – 9256.

[75] ROBINSON J T, PERKINS F K, SNOW E S, et al. Reduced graphene oxide molecular sensors[J]. Nano Letters, 2008, 8(10): 3137 – 3140.

[76] LEE J S, JEONG S, KIM D, et al. Improving DMMP (Salin simulant) sensing characteristics of TFQ functionalized graphene chemiresistive sensors[C]//Proceedings of 2017 IEEE 17th International Conference on Nanotechnology (IEEE-NANO), 2017: 675 – 677.

[77] SINGH E, SINGH P, KIM K S, et al. Flexible molybdenum disulfide (MoS_2) atomic layers for wearable electronics and optoelectronics[J]. ACS Applied Materials & Interfaces, 2019, 11(12): 11061 – 11105.

[78] TSAI M Y, TARASOV A, HESABI Z R, et al. Flexible MoS_2 field-effect transistors for gate-tunable piezoresistive strain sensors[J]. ACS Applied Materials & Interfaces, 2015, 7(23): 12850 – 12855.

[79] LI N, WANG Q Q, SHEN C, et al. Large-scale flexible and transparent electronics based on monolayer molybdenum disulfide field-effect transistors[J]. Nature Electronics, 2020, 3(11): 711 – 717.

[80] ZHOU Y, STEWART R. Highly flexible, durable, UV resistant, and electrically conductive graphene based TPU/textile composite sensor[J]. Polymers for Advanced Technologies, 2022, 33(12): 4250 – 4264.

[81] CHAO M Y, WANG Y G, MA D, et al. Wearable MXene nanocomposites-based strain sensor with tile-like stacked hierarchical microstructure for broad-range ultrasensitive sensing[J]. Nano Energy, 2020, 78: 105187.

[82] LU Y M, ZHAO X N, LIN Y, et al. Lightweight MXene/carbon composite foam with hollow skeleton for air-stable, high-temperature-resistant and compressible electromagnetic interference shielding[J]. Carbon, 2023, 206: 375 – 382.

[83] ZHANG Y F, GONG M, WAN P B. MXene hydrogel for wearable electronics[J]. Matter, 2021, 4(8): 2655 – 2658.

[84] HIGASHITARUMIZU N, WANG S, WANG S F, et al. Black phosphorus for mid-infrared optoelectronics: photophysics, scalable processing, and device applications[J]. Nano Letters, 2024, 24(42): 13107 – 13117.

[85] CHEN Z C, JIANG L, SUN J Y, et al. Ultrafast-laser-induced nanostructures with continuously tunable period on Au surface for photoluminescence control in monolayer MoS_2[J]. Laser & Photonics Reviews, 2025, 19(1): 2400715.

[86] AHMAD W, REHMAN M U, PAN L, et al. Ultrasensitive near-infrared polarization photodetectors with violet phosphorus/InSe van der Waals heterostructures[J]. ACS Applied Materials & Interfaces, 2024, 16(15): 19214 – 19224.

[87] WIJAYA T J, HIGASHITARUMIZU N, WANG S F, et al. Mechanically flexible mid-wave infrared imagers using black phosphorus ink films[J]. Nature Communications, 2025, 16(1): 5972.

[88] 贾欣宇, 兰长勇, 李春. 二维材料在红外探测器中的应用最新进展(特邀)[J]. 红外与激光工程, 2022, 51(7): 20220065.
JIA X Y, LAN C Y, LI C. Recent advances in two-dimensional materials in infrared photodetectors (invited)[J]. Infrared and Laser Engineering, 2022, 51(7): 20220065. (in Chinese)

[89] MIN K H, KIM K H, PACK S P. Two-dimensional materials for biosensing: emerging bio-converged strategies for wearable and implantable platforms[J]. Chemosensors, 2025, 13(6): 209.

[90] SENGUPTA J, HUSSAIN C M. MXene-based electrochemical biosensors: advancing detection strategies for biosensing (2020—2024)[J]. Biosensors, 2025, 15(3): 127.

[91] LIU Y, ZHANG Y T, LI Z J, et al. Fast and in-situ electrodeposition of MXene/AuNPs composite for multiplexed and sensitive detection of infectious biomarkers using an electrochemical biosensor[J]. Microchemical Journal, 2024, 207: 112064.

[92] SARKAR D, LIU W, XIE X J, et al. MoS_2 field-effect transistor for next-generation label-free biosensors[J]. ACS Nano, 2014, 8(4): 3992 – 4003.

[93] ZHU C S, XIONG S Y, WANG C X, et al. SERS-based lateral flow immunoassay combined with enzymatic recombinase amplification for quantitative, high-sensitive detection of influenza a virus[J]. ACS Applied Nano Materials, 2024, 7(3): 3373 – 3384.

[94] LI J X, SHEN W Z, LIANG X Y, et al. 2D film-like magnetic SERS tag with enhanced capture and detection abilities for immunochromatographic diagnosis of multiple bacteria[J]. Small, 2024, 20(22): 2310014.

[95] BOLOTSKY A, BUTLER D, DONG C Y, et al. Two-dimensional materials in biosensing and healthcare: from in vitro diagnostics to optogenetics and beyond[J]. ACS Nano, 2019, 13(9): 9781 – 9810.

[96] LEE J H, LOYA P E, LOU J, et al. Dynamic mechanical behavior of multilayer graphene via supersonic projectile penetration[J]. Science, 2014, 346(6213): 1092 – 1096.

[97] LI L H, CERVENKA J, WATANABE K, et al. Strong oxidation resistance of atomically thin boron nitride nanosheets[J]. ACS Nano, 2014, 8(2): 1457 – 1462.

[98] LIU Z, GONG Y J, ZHOU W, et al. Ultrathin high-temperature oxidation-resistant coatings of hexagonal boron nitride[J]. Nature Communications, 2013, 4: 2541.

[99] BIAN F P, HUANG R, LI X B, et al. Facile construction of chestnut-like structural fireproof PDMS/MXene @ BN for advanced thermal management and electromagnetic shielding applications[J]. Advanced Science, 2024, 11(15): 2307482.

[100] WU T, QIU J D, XU W H, et al. Efficient fabrication of flame-retarding silicone rubber/hydroxylated boron nitride nanocomposites based on volumetric extensional rheology[J]. Chemical Engineering Journal, 2022, 435(Part 3): 135154.

[101] DAVESNE A L, LAZAR S, BELLAYER S, et al. Hexagonal boron nitride platelet-based nanocoating for fire protection[J]. ACS Applied Nano Materials, 2019, 2(9): 5450 – 5459.

[102] ZHU X B, YAN Q Q, CHENG L, et al. Self-alignment of cationic graphene oxide nanosheets for anticorrosive reinforcement of epoxy coatings[J]. Chemical Engineering Journal, 2020, 389: 124435.

[103] LIU M K, LIU X B, WANG S Q, et al. A review on high-performance conductive anti-corrosion coatings: from material innovations to practical implementation[J]. Journal of Applied Polymer Science, 2026, 143(5): e58153.

[104] SUN T Y, HAO Y, WU Y H, et al. Corrosion resistance of ultrathin two-dimensional coatings: first-principles calculations towards in-depth mechanismunderstanding and precise material design[J]. Metals, 2021, 11(12): 2011.

[105] CHEN S S, BROWN L, LEVENDORF M, et al. Oxidation resistance of graphene-coated Cu and Cu/Ni alloy[J]. ACS Nano, 2011, 5(2): 1321 – 1327.

[106] HUSAIN E, NARAYANAN T N, TAHA-TIJERINA J J, et al. Marine corrosion protective coatings of hexagonal boron nitride thin films on stainless steel[J]. ACS Applied Materials & Interfaces, 2013, 5(10): 4129 – 4135.

[107] FAN X Q, YAN H, CAI M, et al. Achieving parallelly-arranged $Ti_3C_2T_x$ in epoxy coating for anti-corrosive/wear high-efficiency protection[J]. Composites Part B Engineering, 2022, 231: 109581.

[108] KUMAR N, AEPURU R, LEE S Y, et al. Recent advances in phosphorene: a promising material for supercapacitor applications[J]. Materials Science and Engineering: R: Reports, 2025, 163: 100932.

[109] ZHANG J P, CHUL L, LIU T J, et al. Engineering spacer conjugation for efficient and stable 2D/3D perovskite solar cells and modules[J]. Angewandte Chemie International Edition, 2025, 64(1): e202413303.

[110] ZHANG Z, LEI B L, TAN Y G, et al. Heterojunctions based on 2D materials for pulse laser applications[J]. ACS Nano, 2025, 19(13): 12646 – 12679.

[111] TAN Y B, LEE J M. Graphene for supercapacitor applications[J]. Journal of Materials Chemistry A, 2013, 1(47): 14814 – 14843.

[112] KE Q Q, WANG J. Graphene-based materials for supercapacitor electrodes: a review[J]. Journal of Materiomics, 2016, 2(1): 37 – 54.

[113] WANG Y, SHI Z Q, HUANG Y, et al. Supercapacitor devices based on graphene materials[J]. Journal of Physical Chemistry C, 2009, 113(30): 13103 – 13107.

[114] LIU C G, YU Z N, NEFF D, et al. Graphene-based supercapacitor with an ultrahigh energy density[J]. Nano Letters, 2010, 10(12): 4863 – 4868.

[115] ZHANG L L, ZHOU R, ZHAO X S. Graphene-based materials as supercapacitor electrodes[J]. Journal of Materials Chemistry, 2010, 20(29): 5983 – 5992.

[116] MISHRA A K, RAMAPRABHU S. Functionalized graphene-based nanocomposites for supercapacitor application[J]. Journal of Physical Chemistry C, 2011, 115(29): 14006 – 14013.

[117] CAO X H, SHI Y M, SHI W H, et al. Preparation of novel 3D graphene networks for supercapacitor applications[J]. Small, 2011, 7(22): 3163 – 3168.

[118] DOWN M P, ROWLEY-NEALE S J, SMITH G C, et al. Fabrication of graphene oxide supercapacitor devices[J]. ACS Applied Energy Materials, 2018, 1(2): 707 – 714.

[119] ZHANG F, ZHANG T F, YANG X, et al. A high-performance supercapacitor-battery hybrid energy storage device based on graphene-enhanced electrode materials with ultrahigh energy density[J]. Energy & Environmental Science, 2013, 6(5): 1623 – 1632.

[120] LI C M, LI X M, YANG Q Z, et al. Vascular system inspired 3D electrolyte network for high rate and high mass loading graphene supercapacitor[J]. Advanced Functional Materials, 2024, 34(26): 2315137.

[121] GE K, WANG Z H, LIU J, et al. Constructing LiF-enriched solid electrolyte interface on graphene arrays with abundant edges on microscale Si-C anodes toward high-energy lithium-ion batteries[J]. Advanced Functional Materials, 2025, 35(5): 2414384.

[122] FAN W, WANG Q, RONG K, et al. MXene enhanced 3D needled waste denim felt for high-performance flexible supercapacitors[J]. Nano-Micro Letters, 2024, 16(1): 36.

[123] YU J Y, QU D Y, WANG X J, et al. A supercapacitor driven by MXene nanofluid gel electrolyte induced the synergistic high ionic migration rate and excellent mechanical properties[J]. Advanced Functional Materials, 2025, 35(6): 2414934.

[124] CHEN Y C, YANG H C, HAN Z J, et al. MXene-based electrodes for supercapacitor energy storage[J]. Energy & Fuels, 2022, 36(5): 2390 – 2406.

[125] JIANG Q, KURRA N, ALHABEB M, et al. All pseudocapacitive MXene-RuO_2 asymmetric supercapacitors[J]. Advanced Energy Materials, 2018, 8(13): 1703043.

[126] ZHAO T Y, YANG D Z, LI B X, et al. A supercapacitor architecture for extreme low-temperature operation featuring MXene/carbon nanotube electrodes with vertically aligned channels and a novel freeze-resistant electrolyte[J]. Advanced Functional Materials, 2024, 34(24): 2314825.

[127] CAI H, ZHANG P K, LI B W, et al. High-entropy oxides for energy-related electrocatalysis[J]. Materials Today Catalysis, 2024, 4: 100039.

[128] ZHU S Y, NONG W, NICHOLAS L J J, et al. Rapid in situ growth of high-entropy oxide nanoparticles with reversible spinel structures for efficient Li storage[J]. Journal of Materials Chemistry A, 2024, 12(19): 11473 – 11486.

[129] ZHU S Y, NONG W, HUANG L, et al. Carbothermal synthesis of high-entropy layered oxides for advanced submicron-particle lithium cathodes[J]. ACS Nano, 2025, 19(38): 34030 – 34041.

[130] MANSOURI S, DEHIMI L, BENCHERIF H, et al. Theoretical simulation on enhancing the thin-film copper zinc tin sulfide solar cell performance using MoS_2, MoO_x, and CuI as efficient hole transport layers[J]. Energy & Fuels, 2024, 38(9): 8187 – 8198.

[131] LI B X, WANG Y L, GU W D, et al. Integration of 2D materials for high performance perovskite solar cells[J]. Nanoscale, 2025, 17(38): 22033 – 22049.

[132] KARIMIPOUR M, KHAZRAEI S, KIM B J, et al. Efficient and bending durable flexible perovskite solar cells via interface modification using a combination of thin MoS_2 nanosheets and molecules binding to the perovskite[J]. Nano Energy, 2022, 95: 107044.

[133] WANG T Y, ZHENG F Y, TANG G Q, et al. 2D WSe_2 flakes for synergistic modulation of grain growth and charge transfer in tin-based perovskite solar cells[J]. Advanced Science, 2021, 8(11): 2004315.

[134] YIN Y F, ZHOU Y C, FU S, et al. Template-assisted growth of high-quality α-phase $FAPbI_3$ crystals in perovskite solar cells using thiol-functionalized MoS_2 nanosheets[J]. ACS Nano, 2024, 18(44): 30816 – 30828.

[135] DONG H Y, FAN J Y, FANG H H, et al. Modification at ITO/NiO_x interface with MoS_2 enables hole transport for efficient and stable inverted perovskite solar cells[J]. ChemSusChem, 2025, 18(10): e202402400.

[136] XIA J M, LIANG C, GU H, et al. Two-dimensional heterostructure of MoS_2/BA_2PbI_4 2D Ruddlesden-popper perovskite with an S scheme alignment for solar cells: a first-principles study[J]. ACS Applied Electronic Materials, 2022, 4(4): 1939 – 1948.

[137] GOLDREICH A, PRILUSKY J, PRASAD N, et al. Highly stable $CsPbBr_3$ @ MoS_2 nanostructures: synthesis and optoelectronic properties toward implementation into solar cells[J]. Small, 2024, 20(45): 2404727.

[138] TAN C, TAO R, YANG Z H, et al. Tune the photoresponse of monolayer MoS_2 by decorating $CsPbBr_3$ perovskite nanoparticles[J]. Chinese Chemical Letters, 2023, 34(7): 107979.

[139] JUNG D H, OH Y J, NAM Y S, et al. Effect of layer

number on the properties of stable and flexible perovskite solar cells using two dimensional material[J]. Journal of Alloys and Compounds, 2021, 850: 156752.

[140] KIM B, KIM M, KIM H, et al. Improved stability of $MAPbI_3$ perovskite solar cells using two-dimensional transition-metal dichalcogenide interlayers[J]. ACS Applied Materials & Interfaces, 2022, 14(31): 35726 – 35733.

[141] WU M, LI W Z, HU R Q, et al. Electrostatic shielding to stabilize buried interface toward high-performance inorganic perovskite solar cells[J]. Small Methods, 2026, 10(2): 2500554.

[142] CAPASSO A, MATTEOCCI F, NAJAFI L, et al. Few-layer MoS_2 flakes as active buffer layer for stable perovskite solar cells[J]. Advanced Energy Materials, 2016, 6(16): 1600920.

[143] NAJAFI L, TAHERI B, MARTÍN-GARCÍA B, et al. MoS_2 quantum dot/graphene hybrids for advanced interface engineering of a $CH_3NH_3PbI_3$ perovskite solar cell with an efficiency of over 20[J]. ACS Nano, 2018, 12(11): 10736 – 10754.

[144] SINGH R, GIRI A, PAL M, et al. Perovskite solar cells with an MoS_2 electron transport layer[J]. Journal of Materials Chemistry A, 2019, 7(12): 7151 – 7158.

[145] KOHNEHPOUSHI S, NAZARI P, NEJAND B A, et al. MoS_2: a two-dimensional hole-transporting material for high-efficiency, low-cost perovskite solar cells[J]. Nanotechnology, 2018, 29(20): 205201.

[146] SINGH E, KIM K S, YEOM G Y, et al. Atomically thin-layered molybdenum disulfide (MoS_2) for bulk-heterojunction solar cells[J]. ACS Applied Materials & Interfaces, 2017, 9(4): 3223 – 3245.

[147] PENG B, YU G N, ZHAO Y W, et al. Achieving ultrafast hole transfer at the monolayer MoS_2 and $CH_3NH_3PbI_3$ perovskite interface by defect engineering[J]. ACS Nano, 2016, 10(6): 6383 – 6391.

[148] ZAI H C, YANG P F, SU J, et al. Wafer-scale monolayer MoS_2 film integration for stable, efficient perovskite solar cells[J]. Science, 2025, 387(6730): 186 – 192.

[149] KOO D, CHOI Y, KIM U, et al. Mesoporous structured MoS_2 as an electron transport layer for efficient and stable perovskite solar cells[J]. Nature Nanotechnology, 2025, 20(1): 75 – 82.

[150] 胡知力, 薛敏珉, 赵志强, 等. 二维材料曲面生长: 力学与化学的邂逅[J]. 计算力学学报, 2021, 38(3): 321 – 326.
HU Z L, XUE M M, ZHAO Z Q, et al. 2D materials growth on curved surfaces: when mechanics meets chemistry[J]. Chinese Journal of Computational Mechanics, 2021, 38(3): 321 – 326. (in Chinese)

[151] HE C J, XU C, CHEN C, et al. Unusually high thermal conductivity in suspended monolayer $MoSi_2N_4$[J]. Nature Communications, 2024, 15(1): 4832.

[152] HE M K, ZHONG X, LU X H, et al. Excellent low-frequency microwave absorption and high thermal conductivity in polydimethylsiloxane composites endowed by hydrangea-like CoNi @ BN heterostructure fillers[J]. Advanced Materials, 2024, 36(48): 2410186.

[153] CHEN D K, CAI H, XUAN X Y, et al. Data-driven description of the lattice thermal conductivity of two-dimensional materials[J]. Journal of Physical Chemistry Letters, 2025, 16(32): 8165 – 8172.

[154] HE Y M, CLARK G, SCHAIBLEY J R, et al. Single quantum emitters in monolayer semiconductors[J]. Nature Nanotechnology, 2015, 10(6): 497 – 502.

[155] SRIVASTAVA A, SIDLER M, ALLAIN A V, et al. Optically active quantum dots in monolayer WSe_2[J]. Nature Nanotechnology, 2015, 10(6): 491 – 496.

[156] KOPERSKI M, NOGAJEWSKI K, ARORA A, et al. Single photon emitters in exfoliated WSe_2 structures[J]. Nature Nanotechnology, 2015, 10(6): 503 – 506.

[157] JUNGWIRTH N R, CALDERON B, JI Y X, et al. Temperature dependence of wavelength selectable zero-phonon emission from single defects in hexagonal boron nitride[J]. Nano Letters, 2016, 16(10): 6052 – 6057.

[158] GAO T, VON HELVERSEN M, ANTÓN-SOLANAS C, et al. Atomically-thin single-photon sources for quantum communication[J]. npj 2D Materials and Applications, 2023, 7(1): 4.

[159] ZHAO H, PETTES M T, ZHENG Y, et al. Site-controlled telecom-wavelength single-photon emitters in atomically-thin $MoTe_2$[J]. Nature Communications, 2021, 12(1): 6753.

[160] CHAKRABORTY C, KINNISCHTZKE L, GOODFELLOW K M, et al. Voltage-controlled quantum light from an atomically thin semiconductor[J]. Nature Nanotechnology, 2015, 10(6): 507 – 511.

[161] PALACIOS-BERRAQUERO C. Atomically-thin quantum light emitting diodes[M]//Quantum Confined Excitons in 2-Dimensional Materials. Berlin: Springer, 2018: 71 – 89.

[162] YU L, DENG M D, ZHANG J L, et al. Site-controlled quantum emitters in monolayer $MoSe_2$[J]. Nano Letters, 2021, 21(6): 2376 – 2381.

[163] XU X D, YAO W, XIAO D, et al. Spin and pseudospins in layered transition metal dichalcogenides[J]. Nature Physics, 2014, 10(5): 343 – 350.

[164] MAK K F, HE K L, SHAN J, et al. Control of valley polarization in monolayer MoS_2 by optical helicity[J]. Nature Nanotechnology, 2012, 7(8): 494 – 498.

[165] XUE Y Z, WANG H, TAN Q H, et al. Anomalous pressure characteristics of defects in hexagonal boron nitride flakes[J]. ACS Nano, 2018, 12(7): 7127 – 7133.

[166] GUPTA S, YANG J H, YAKOBSON B I. Two-level quantum systems in two-dimensional materials for single photon emission[J]. Nano Letters, 2019, 19(1): 408 – 414.

[167] ZHOU X C, ZHANG Z H, GUO W L. Dislocations as single photon sources in two-dimensional semiconductors[J]. Nano Letters, 2020, 20(6): 4136 – 4143.

[168] GUPTA S, WU W J, HUANG S X, et al. Single-photon emission from two-dimensional materials, to a brighter future[J]. The Journal of Physical Chemistry Letters, 2023, 14(13): 3274 – 3284.

[169] PAN C, WANG C Y, LIANG S J, et al. Reconfigurable logic and neuromorphic circuits based on electrically tunable two-dimensional homojunctions[J]. Nature Electronics, 2020, 3(7): 383 – 390.

[170] WANG S, PAN X, LYU L Y, et al. Nonvolatile van der Waals heterostructure phototransistor for encrypted optoelectronic logic circuit[J]. ACS Nano, 2022, 16(3): 4528 – 4535.

[171] SUN L F, YAN J X, ZHAN D, et al. Spin-orbit splitting in

single-layer MoS_2 revealed by triply resonant Raman scattering[J]. Physical Review Letters, 2013, 111(12): 126801.

[172] ZHU X J, LI D, LIANG X G, et al. Ionic modulation and ionic coupling effects in MoS_2 devices for neuromorphic computing[J]. Nature Materials, 2019, 18(2): 141 – 148.

[173] ZHANG F, ZHANG H R, KRYLYUK S, et al. Electric-field induced structural transition in vertical $MoTe_2$- and $Mo_{1-x}W_xTe_2$-based resistive memories[J]. Nature Materials, 2019, 18(1): 55 – 61.

[174] KWON K C, ZHANG Y S, WANG L, et al. In-plane ferroelectric tin monosulfide and its application in a ferroelectric analog synaptic device[J]. ACS Nano, 2020, 14(6): 7628 – 7638.

[175] WANG L, WANG X J, ZHANG Y S, et al. Exploring ferroelectric switching in α-In_2Se_3 for neuromorphic computing [J]. Advanced Functional Materials, 2020, 30(45): 2004609.

[176] JANG B C, KIM S, YANG S Y, et al. Polymer analog memristive synapse with atomic-scale conductive filament for flexible neuromorphic computing system[J]. Nano Letters, 2019, 19(2): 839 – 849.

[177] WU X H, GE R J, CHEN P A, et al. Thinnest nonvolatile memory based on monolayer h-BN[J]. Advanced Materials, 2019, 31(15): 1806790.

[178] VU Q A, SHIN Y S, KIM Y R, et al. Two-terminal floating-gate memory with van der Waals heterostructures for ultrahigh on/off ratio[J]. Nature Communications, 2016, 7(1): 12725.

[179] GUO J, WANG L Y, LIU Y, et al. Highly reliable low-voltage memristive switching and artificial synapse enabled by van der Waals integration[J]. Matter, 2020, 2(4): 965 – 976.

[180] WANG M, CAI S H, PAN C, et al. Robust memristors based on layered two-dimensional materials [J]. Nature Electronics, 2018, 1(2): 130 – 136.

[181] PACAKOVA B, LAHTINEN-DAHL B, KIRCH A, et al. Naturally occurring 2D semiconductor with antiferromagnetic ground state[J]. npj 2D Materials and Applications, 2025, 9(1): 38.

[182] ESRF. Clay emerges as a natural semiconductor[EB/OL]. [2025 – 12 – 28]. https://www.esrf.fr/cms/live/live/en/sites/www/home/news/general/content-news/general/clay-emerges-as-a-natural-semiconductor.html.

[183] HUANG L, CAO Y Z, QIU H S, et al. Terahertz oscillation driven by optical spin-orbit torque [J]. Nature Communications, 2024, 15(1): 7227.

[184] VOGL T, SRIPATHY K, SHARMA A, et al. Radiation tolerance of two-dimensional material-based devices for space applications[J]. Nature Communications, 2019, 10(1): 1202.

[185] ARNOLD A J, SHI T, JOVANOVIC I, et al. Extraordinary radiation hardness of atomically thin MoS_2[J]. ACS Applied Materials & Interfaces, 2019, 11(8): 8391 – 8399.

[186] SHI L. Challenges remain for 2D semiconductor growth[J]. Nature Nanotechnology, 2024, 19(2): 145.

[187] LI J Z, CHEN M G, SAMAD A, et al. Wafer-scale single-crystal monolayer graphene grown on sapphire substrate[J]. Nature Materials, 2022, 21(7): 740 – 747.

[188] CANTO B, OTTO M, MAESTRE A, et al. Multi-project wafer runs for electronic graphene devices in the European 2D-experimental pilot line project [J]. Nature Communications, 2025, 16(1): 1417.

[189] SONG S, JEON S, RAHAMAN M, et al. Wafer-scale growth of two-dimensional, phase-pure InSe[J]. Matter, 2023, 6(10): 3483 – 3498.

[190] XIA Y, CHEN X Y, WEI J C, et al. 12-inch growth of uniform MoS_2 monolayer for integrated circuit manufacture[J]. Nature Materials, 2023, 22(11): 1324 – 1331.

[191] LEMME M C, DAUS A. Low-temperature MoS_2 growth on CMOS wafers[J]. Nature Nanotechnology, 2023, 18(5): 446 – 447.

[192] LI L, WANG Q Q, WU F F, et al. Epitaxy of wafer-scale single-crystal MoS_2 monolayer via buffer layer control[J]. Nature Communications, 2024, 15(1): 1825.

[193] SHEN P C, SU C, LIN Y X, et al. Ultralow contact resistance between semimetal and monolayer semiconductors[J]. Nature, 2021, 593(7858): 211 – 217.

[194] LIU Y, GUO J, ZHU E B, et al. Approaching the Schottky-Mott limit in van der Waals metal-semiconductor junctions[J]. Nature, 2018, 557(7707): 696 – 700.

[195] YUE M, ZHANG K N, ZHAO M, et al. 2D Cd metal contacts via low-temperature van der Waals epitaxy towards high-performance 2D transistors [J]. Nature Communications, 2025, 16(1): 4018.

[196] KONG L G, WU R X, CHEN Y, et al. Wafer-scale and universal van der Waals metal semiconductor contact[J]. Nature Communications, 2023, 14(1): 1014.

[197] YUAN G W, LIU W L, HUANG X L, et al. Stacking transfer of wafer-scale graphene-based van der Waals superlattices[J]. Nature Communications, 2023, 14(1): 5457.

[198] LIU C, LI Z H, QIAO R X, et al. Designed growth of large bilayer graphene with arbitrary twist angles [J]. Nature Materials, 2022, 21(11): 1263 – 1268.

[199] FAVRON A, GAUFRÈS E, FOSSARD F, et al. Photooxidation and quantum confinement effects in exfoliated black phosphorus[J]. Nature Materials, 2015, 14(8): 826 – 832.

[200] YANG J Q, LIU X C, DONG Q L, et al. Oxidations of two-dimensional semiconductors: fundamentals and applications[J]. Chinese Chemical Letters, 2022, 33(1): 177 – 185.

[201] GB/T 30544.13—2018. 纳米科技 术语 第13部分：石墨烯及相关二维材料[S]. 北京：中国标准出版社，2018.
GB/T 30544.13—2018. Nanotechnologies—vocabulary—part 13: graphene and related two-dimensional (2D) materials[S]. Beijing: Standards Press of China, 2018. (in Chinese)

[202] T/CSTM 00166.1—2020. 石墨烯材料表征 第1部分：拉曼光谱法[S]. 北京：中关村材料试验技术联盟，2020.
T/CSTM 00166.1—2020. Characterization for graphene materials—part 1: Raman spectroscopy [S]. Beijing: Zhongguancun Materials Testing Technology Alliance, 2020. (in Chinese)

[203] T/CGIA 002—2018. 含有石墨烯材料的产品命名指南[S]. 北京：中国石墨烯产业技术创新战略联盟，中关村华清石墨烯产业技术创新联盟，2018.
T/CGIA 002—2018. Guidance on naming of products

containing graphene materials[S]. Beijing: China Graphene Industry Technology Innovation Strategic Alliance, Zhongguancun Huaqing Graphene Industry Technology Innovation Alliance, 2018. (in Chinese)

[204] QJ 1558B—2016. 真空条件下材料挥发性能测试方法[S]. 北京: 国家国防科技工业局, 2016.
QJ 1558B—2016. Test method for materials outgassing performance in vacuum [S]. Beijing: National Defense Science and Technology Industry Bureau, 2016. (in Chinese)

[205] GJB 548C—2021. 微电子器件试验方法和程序[S]. 北京: 中央军委装备发展部, 2021.
GJB 548C—2021. Test methods and procedures for microelectronic devices [S]. Beijing: Equipment Development Department of the Central Military Commission, 2021. (in Chinese)

[206] GJB 360B—2009. 电子及电气元件试验方法[S]. 北京: 中国人民解放军总装备部, 2009.
GJB 360B—2009. Test methods for electronic and electrical component pasrts [S]. Beijing: General Equipment Department of the Chinese People's Liberation Army, 2009. (in Chinese)

[207] GJB 150.1A—2009. 军用装备实验室环境试验方法 第1部分: 通用要求[S]. 北京: 中国人民解放军总装备部, 2009.
GJB 150.1A—2009. Laboratory environmental test methods for military materiel—part 1: general requirements [S]. Beijing: General Equipment Department of the Chinese People's Liberation Army, 2009. (in Chinese)

[208] GB/T 2423.1—2008. 电工电子产品环境试验 第2部分: 试验方法 试验 A: 低温[S]. 北京: 中国标准出版社, 2008.
GB/T 2423.1—2008. Environmental testing—part 2: test methods—tests A: cold [S]. Beijing: Standards Press of China, 2008. (in Chinese)

[209] GJB 151B—2013. 军用设备和分系统电磁发射和敏感度要求与测量[S]. 北京: 中国人民解放军总装备部, 2013.
GJB 151B—2013. Electromagnetic emission and susceptibility requirements and measurements for military equipment and subsystems[S]. Beijing: General Equipment Department of the Chinese People's Liberation Army, 2013. (in Chinese)

[210] GJB/Z 24A—2020. 地球辐射带[S]. 北京: 中央军委装备发展部, 2020.
GJB/Z 24A—2020. Earth's radiation belt [S]. Beijing: Equipment Development Department of the Central Military Commission, 2020. (in Chinese)

[211] GJB 7242—2011. 单粒子效应试验方法和程序[S]. 北京: 中国人民解放军总装备部, 2011.
GJB 7242—2011. Test methods and procedures for single-event effects[S]. Beijing: General Equipment Department of the Chinese People's Liberation Army, 2011. (in Chinese)

[212] QJ 10005—2008. 宇航用半导体器件重离子单粒子效应试验指南[S]. 北京: 国防科学技术工业委员会, 2008.
QJ 10005—2008. Test guidelines of single event effects induced by heavy ions of semiconductor devices for space applications [S]. Beijing: National Defense Science, Technology and Industry Committee, 2008. (in Chinese)

[213] GJB 2502.6—2006. 航天器热控涂层试验方法 第6部分: 真空-质子辐照试验[S]. 北京: 国防科学技术工业委员会, 2006.
GJB 2502.6—2006. Test method for thermal control coatings of spacecraft—part 6: proton irradiation test in vacuum [S]. Beijing: National Defense Science, Technology and Industry Committee, 2006. (in Chinese)

[214] 沈自才, 闫德葵. 空间辐射环境工程的现状及发展趋势[J]. 航天器环境工程, 2014, 31(3): 229-240.
SHEN Z C, YAN D K. Present status and prospects of space radiation environmental engineering [J]. Spacecraft Environment Engineering, 2014, 31(3): 229-240. (in Chinese)